

UNIVERSITY OF MICHIGAN RESEARCH INSTITUTE  
THE UNIVERSITY OF MICHIGAN  
ANN ARBOR

STANDING WAVE MEASUREMENTS IN COAXIAL SYSTEMS

Technical Report No. 87  
Electronic Defense Group  
Department of Electrical Engineering

By: W. M. Nunn, Jr.

Approved by: *C. B. Sharpe*  
C. B. Sharpe

Project 2262

TASK ORDER NO. EDG-4  
CONTRACT NO. DA-36-039 sc-63203  
SIGNAL CORPS, DEPARTMENT OF THE ARMY  
DEPARTMENT OF ARMY PROJECT NO. 3-99-04-042  
SIGNAL CORPS PROJECT NO. 194B

September 1958

### ACKNOWLEDGEMENT

The author wishes to express his appreciation to Dr. P.D. Lacy of the Hewlett-Packard company and to Mr. R.W. Beatty of the National Bureau of Standards for their constructive criticism of certain aspects of the measurement procedure.

## TABLE OF CONTENTS

	Page
LIST OF ILLUSTRATIONS	iv
LIST OF TABLES	iv
LIST OF SYMBOLS	v
ABSTRACT	vii
1. INTRODUCTION	1
1.1 Microwave Impedance Measurement Techniques	4
1.1.1 The Slotted Line Method	4
1.1.2 The Resonance-Curve Method	6
1.1.3 The Microwave Bridge Method	8
1.1.4 The MacPherson-Kerns Method	8
1.1.5 The Double-Slug Transformer Method	9
1.1.6 The Reflectometer Method	10
1.2 Standing Wave Ratio Measurement Techniques	11
1.2.1 The Direct Method	11
1.2.2 The Small Reflection Method	12
1.2.3 The Roberts-von Hippel Method	14
1.2.4 The Shunt Method	16
1.2.5 The Winzemer Method	16
1.2.6 The Substitution Method	18
2. DERIVATION OF THE GENERAL RELATIONS	22
2.1 The Vector Relations in Lossless Systems	22
2.2 Selection of Coordinate Reference	24
2.2.1 The Standing Wave Maximum	25
2.2.2 The Standing Wave Minimum	28
2.3 Table of Standing Wave Relations	28
2.4 An Important Special Case	30
2.5 Relation Between VSWR, Wavelength and Twice Power Points	33
3. THE MEASUREMENT PROCEDURE	36
3.1 The Matching Technique	36
3.2 The Experimental Verification	41
4. ANALYSIS OF ERRORS	44
4.1 Fundamental Error Sources in Physical Measurements	44
4.2 Characteristics of the Slotted Line	45
4.2.1 Probe and Slot Effects	45
4.3 Errors Affecting the RF Substitution Method	51
4.3.1 Mismatch Errors	52
4.3.2 Attenuation, Angle and Wavelength Errors	57
4.4 Effects of Frequency Drift	59
REFERENCES	61
DISTRIBUTION LIST	67

## LIST OF ILLUSTRATIONS

Figure		Page
1	Conditions Existing Near a Standing Wave Minimum	14
2	Substitution Methods for Measuring Standing Wave Ratio	19
3	The Representation of Lossless Transmission Systems	23
4	Vector Relations for a Standing Wave Maximum and Minimum	25
5	Definition of the Electrical Angles	26
6	Voltage Standing Wave Ratio Versus Normalized Displacement from the Position of the Minimum	31
7	Relation Between VSWR, Wavelength and Twice Power Points	34
8	Standing Wave Measurement Equipment	37
9	Block Diagram Representation of RF Substitution Method of Measuring Standing Wave Ratio	53

## LIST OF TABLES

I	The Standing Wave Relations	29
II	Parameter Variation Test	42
III	Comparison Test	43
IV	Standing Wave Ratio Uncertainty	58

## LIST OF SYMBOLS

A	Arbitrary angle (equation 5)
d	Distance between which the power is twice the value at a standing wave minimum (Fig. 7)
$I_{\max}$	Rectified current observed at a standing wave maximum (equation 7)
$I_{\min}$	Rectified current observed at a standing wave minimum (equation 7)
K	A constant quantity (equation 6)
$K^2$	A constant quantity (equation 12)
L	Insertion loss (equation 28)
$l$	Length of transmission line between source and load (Fig. 3)
$S_{11}, S_{12}, S_{22}$	Coefficients of the scattering matrix (Fig. 9)
$V_i$	Incident voltage, including magnitude and phase angle
$V_{\max}$	Voltage at a standing wave maximum
$V_{\min}$	Voltage at a standing wave minimum
$V_r$	Reflected voltage, including magnitude and phase angle
w	The distance between equal response points above a standing wave minimum (Fig. 1)
x	A one-dimensional space variable (Fig. 3)
$x_{\min}$	The value at x at a standing wave minimum (Fig. 1)
$x_0$	The distance between a standing wave minimum and the point where the power is twice the minimum value (Fig. 7)
z	Normalized load impedance (equation 3)
$Z_g$	Source impedance, including magnitude and phase angle, in ohms (Fig. 3)

$Z_L$	Load impedance, including magnitude and phase angle, in ohms (equation 3)
$Z_0$	Characteristic impedance of transmission line, in ohms (equation 3)
$\alpha$	A quantity defined according to equation 19
$\beta$	Phase constant in the transmission line ( $= 2\pi/\lambda$ ), in radians per meter
$\Gamma$	Complex reflection coefficient at an arbitrary reference plane
$\Gamma_G$	Complex reflection coefficient of the signal source
$\Gamma_L$	Complex reflection coefficient of the load
$\delta$	An angle defined according to Fig. 5
$\epsilon$	Fractional error in standing wave measurement (equation 27)
$\theta$	An angle defined according to equation 15
$\theta_0$	An angle defined according to Fig. 5
$\lambda$	Wavelength in the transmission system, in meters
$\pi$	Ratio of circumference to the diameter of a circle
$\rho$	Voltage standing wave ratio
$\phi$	Phase angle of the load reflection coefficient
$\psi$	Angle defined as in Fig. 3
$\ln x$	The natural logarithm of x
$\log_{10}x$	The common logarithm of x
$ x $	The magnitude of x
$\Delta x$	The incremental change in x
$\approx$	Symbol used to indicate that the left member of an equation is approximately equal to the right member of the same equation
$\triangleq$	Symbol used to indicate that the left member of an equation is equal by definition to the right member of the same equation

## ABSTRACT

The material presented in this report describes an investigation undertaken to accurately measure large standing wave ratios in lossless coaxial transmission systems. The study was divided into three parts: (1) a literature review; (2) a theoretical analysis; and (3) the development of an experimental procedure.

A brief review of the existing methods for determining microwave impedance and standing wave ratio is described first. This is followed by a derivation of the general relations which lead to several important special cases. A description of the experimental procedure is given, after which an analysis of errors is presented.





## STANDING WAVE MEASUREMENTS IN COAXIAL SYSTEMS

### 1. INTRODUCTION

The impedance concept is generally recognized (Ref. 25) as a fundamental entity relating cause and effect in many physical systems. It is therefore natural that the subject of impedance measurement should occupy a dominant role in all phases of electrical engineering. In the low frequency range of the electromagnetic spectrum a number of highly refined procedures have been developed for the precise measurement of the impedance of passive circuit elements.

Below several tens of cycles, for example, a combination of voltmeters, ammeters and wattmeters may be employed in the measurement of circuit parameters. As the frequency is raised, certain limitations imposed upon the construction of the instruments limit the usefulness of this procedure. However bridge circuits are commercially available which permit the accurate determination of inductance, resistance and capacity from the low audio frequencies to the radio frequency range. Although special precautions must be taken, very successful bridge circuits have been constructed for frequencies as high as 50 mc. Beyond this range certain difficulties arise concerning a proper interpretation of voltage and current. In addition, the possibility of higher order field configurations, stray coupling and radiation from both the test equipment and the components under investigation become particularly troublesome. In spite of these difficulties one manufacturer has developed a bridge covering the frequency range 50-1000 mc, while another has developed a bridge covering the frequency range 50-500 mc (References 23, 33).

In the microwave range of frequencies certain conventions must be adopted (Ref. 25) concerning the location of the "accessible" circuit terminals and the meaning of the term "impedance." These peculiarities exemplify the electromagnetic character of the phenomena and its physical manifestations. It becomes convenient to treat the electric and magnetic fields present in the

system and to analyze the effects observed in terms of incident and reflected electromagnetic waves. For convenience of measurement, however, these fields are treated in terms of their integrated results, namely voltage and current.

An important quantity in this analysis is the voltage reflection coefficient at the load,  $\Gamma_L$ , which is given by the relation

$$\Gamma_L = \frac{V_r}{V_i} \quad (1)$$

where

$V_r$  = reflected voltage measured at the load, and

$V_i$  = incident voltage measured at the load.

Since  $V_r$  and  $V_i$  are complex quantities possessing both a magnitude and a phase angle, the load reflection coefficient is likewise complex. As long as the magnitudes of these voltages do not change, however, the magnitude of the reflection coefficient remains constant. This condition is assumed to hold in the present treatment as only lossless transmission systems will be considered. Consequently, the reflection coefficient measured at any arbitrary reference plane relative to the load differs from the load reflection coefficient only in its phase angle. Under these circumstances, another useful relation is

$$|\Gamma| = \frac{\rho-1}{\rho+1} \quad (2)$$

where

$|\Gamma|$  = magnitude of the reflection coefficient at any convenient reference plane, and

$\rho \triangleq$  voltage standing wave ratio.\*

In the American literature the voltage standing wave ratio has the accepted meaning of the ratio of the amplitude of the voltage maximum to the amplitude

---

\* The symbol  $\triangleq$  will be used throughout this report to mean that the left member of an equation is equal by definition to the right member of the same equation.

of the voltage minimum on a standing wave. The abbreviation VSWR is often used when referring to this quantity.

A third important relation is the normalized load impedance,  $z$ ,

$$\begin{aligned} z &= \frac{Z_L}{Z_0} \\ &= \frac{1 + \Gamma_L}{1 - \Gamma_L} \quad , \end{aligned} \quad (3)$$

where

$Z_L$  = load impedance in ohms, and

$Z_0$  = characteristic impedance of the transmission line in ohms.

In lossless transmission systems the characteristic impedance is a real number so that the normalization indicated above is quite simple.

It is clear from a study of the foregoing relations that microwave networks may be specified either in terms of their impedance or reflection coefficient. Each designation requires two items of information for the complete description. Thus, the magnitude and the phase angle of the load reflection coefficient can be given, or the real and imaginary parts of the normalized load impedance provide the required information. Moreover, conversion from impedance to reflection coefficient can be readily accomplished by means of the Smith chart. This device is also particularly useful for determining the impedance looking into the terminals of an arbitrary reference plane of a lossless transmission line, when the load impedance and the location of the reference plane relative to the load are known quantities. In view of these considerations, the measurement of the complex reflection coefficient at an arbitrary reference plane a known distance from the load is equivalent to measuring either the load reflection coefficient or the load impedance.

The relationship between the magnitude of the load reflection coefficient and the VSWR given by equation (2) thus provides one of the required items of information necessary for the complete specification of the impedance. The purpose of this report is to present a detailed treatment of one precision method for measuring large standing wave ratios. In order to bring this work

into proper perspective several important microwave impedance measurement procedures are briefly described, after which existing VSWR measurement techniques are summarized.

## 1.1 Microwave Impedance Measurement Techniques

1.1.1 The Slotted Line Method. The slotted line has been extensively used for the measurement of impedance in the VHF and microwave frequency ranges for many years (References 6, 18, 25, 35, 36, 45, 59, 63). The method consists of inserting a slotted section of transmission line between the generator and the load whose impedance is to be determined. Whenever the load impedance differs from the characteristic impedance of the line, reflections are produced at the load which interact with the incident waves, resulting in standing waves. The standing wave ratio measurement provides a direct indication of the magnitude of the load reflection coefficient. Also, the amount that the standing wave minimum shifts (in the presence of the load) with respect to some known reference point (for example, the location of a minimum produced by a short circuit) is a measure of the phase angle of the load reflection coefficient. Moreover, a method for measuring the coefficients of the scattering matrix of the microwave structure has been presented by Deschamps (Ref. 17) which only requires the use of a sliding short circuit affixed to the slotted line and a suitable method of measuring VSWR. In addition, Oliner and Felsen have developed methods for measuring the equivalent circuit parameters of passive microwave structures using similar techniques (References 25, 32). Slotted lines have thus become a most important instrument in the measurement of load reflection coefficients and microwave circuit impedances.

The standard means for exploring the fields in the slotted line is through the use of a small straight probe inserted in the slot and arranged to move parallel to the lines. From a knowledge of the field configuration present in the system, it is possible to locate the slot in such a manner as to produce a minimum disturbance. The probe is connected to a barretter or crystal rectifier detecting element which delivers its output to a suitable indicating instrument. The reading on the instrument can then be interpreted in terms of the fields which produce it, so that changes which occur on the indicator, as

the probe is moved, can be directly related to the spacial distribution of the fields.

An analysis of the errors and the methods for minimizing them have been treated extensively (References 4, 6, 13, 25, 32, 40, 45, 46, 49, 50, 65, 70, 72, 75, 77). The use of small, properly situated slots in special transmission system geometries, special probe designs and high quality detecting elements have resulted in excellent measurement accuracy over certain dynamic ranges of operation. Furthermore, the range of operation can be readily increased by special measurement techniques (References 38, 39, 77, 78, 79).

All of the measurement procedures described in this chapter are subject to the errors arising from uncontrolled variations in the output power of the signal source. However, the slotted waveguide and coaxial transmission systems afford a simple means for minimizing the effects produced by these fluctuations (Ref. 70). A small fraction of the energy is extracted from the generator by means of a directional coupler and is delivered to a barretter or crystal rectifier which is placed in one arm of a bridge circuit. A similar barretter or crystal is used in the traveling detector that is associated with another arm of the bridge. The circuit is arranged to develop an output when the signals reaching the two detectors are different. Since a given change in source power produces the same change in both detectors simultaneously, uncontrolled signal changes do not affect the readout devices.

Standing wave data can be presented visually by employing a reversible motor-driven mechanism to operate the moving detector with the output appearing on a cathode ray oscilloscope (Ref. 2). This arrangement permits rapid determination of the effect upon standing wave ratio of changes in a given load variable.

The standing wave apparatus has also been modified by replacing the single movable probe with as many as four fixed probes. The use of at least three probes is sufficient to completely determine the complex reflection coefficient (References 12, 25). It is also possible to obtain a visual display of the data by employing a swept frequency source in conjunction with the probes (Ref. 25). However, while the multiple probe device eliminates the necessity for moving parts in the slotted section, more source power will be required than in the case of a single probe, and more attention must be given to the influence of the probes upon the transmission system.

1.1.2 The Resonance-Curve Method. A method of impedance measurement used in the UHF frequency range has been developed by R. A. Chipman (Ref. 14). The apparatus consists of a high frequency transmission system one end of which is terminated in the unknown load. The other extremity contains an adjustable short circuit to which a small loop is attached. Coupling to the magnetic field component provides energy for the detector, the output of which is subsequently amplified and delivered to an indicator. The source supplies energy to the system through a fixed probe located between the load and the adjustable short circuit.

When the movable short circuit is located at integer multiples of half-wavelengths from the fixed probe, it can be considered as appearing directly across the source terminals. The detector reading is then a measure of the generator short circuit current. Displacement of the short circuit from this position, which produces maximum detector current, results in a typical resonance curve. If the detector can be assumed to have a square-law relation between voltage and current the standing wave ratio is given by (Ref. 25)

$$\rho = \sqrt{\frac{2(K-1)}{1 - \cos 2\beta x_k} + 1} \quad (4)$$

where

$\beta = 2\pi/\lambda =$  phase constant in the transmission system in radians per meter,

$\lambda =$  wavelength in the transmission system in meters, and

$K =$  a constant which determines the point  $x_k$  from the resonance curve (References 14, 25).

Using the well known trigonometric relation

$$\cos 2A = 1 - 2 \sin^2 A \quad , \quad (5)$$

equation (4) becomes

$$\rho = \frac{1}{\sin \beta x_k} \sqrt{K - \cos^2 \beta x_k} \quad . \quad (6)$$

Since the detector output is a maximum when the short circuit is an integer multiple of half-wavelengths from the source, the location of peak

response determines the position at which the load can be replaced by a pure resistance  $Z_0/\rho$ . The load impedance may then be obtained by transforming this pure resistance through an electrical angle equal to its distance from the load.

Although the positions of the source and the detector may be interchanged, it is significant to observe that the maximum height of the observed resonance curve, at each integer multiple of a half-wavelength between the source and the short circuit, is largest when the configuration first described is employed.\* This is easily seen to follow from the fact that the detector terminals are then always located at a point of maximum magnetic field intensity since the maximum current flows through the short circuit.

When the location of the source and detector are interchanged the height of the observed resonance curve depends upon the intensity of the field sampled, and is a maximum only when the detector is located at the point of maximum field intensity.

Nevertheless, either arrangement permits the application of equation (6) since only relative magnitudes are important in determining the standing wave ratio. Furthermore, as long as the transmission system and the short circuit are perfectly lossless, the maximum height of the resonance curve is constant and independent of the particular half-wavelength multiple at which the detector indicates a peak response.

While this method avoids errors due to the slot and variable probe coupling present in slotted lines (References 45, 72, 73, 75), both the source and the detector must be very loosely coupled to the transmission system to reduce undesirable loading (Ref. 25). A much larger signal is therefore required from the source than in the slotted line, because the latter permits tight generator coupling to the transmission system. Also, a large source impedance compared to the load impedance leads to serious errors in the resonance-curve method. Finally, the presence of losses in the transmission system and

---

\* It is assumed in the present analysis that the transmission system and the adjustable short circuit are perfectly lossless. The interpretation of the data which applies when these conditions do not hold is discussed in reference 25.

adjustable short circuit lead to errors in the measured VSWR. When these losses are known correction curves may be used to obtain the actual VSWR of the unknown load (References 14, 25).

1.1.3 The Microwave Bridge Method. It was mentioned earlier that bridge circuits, which are so rapid and precise for measuring the impedance of passive circuit elements at low frequencies, are subject to severe limitations at microwave frequencies. Nevertheless bridges have been constructed (Ref. 45) from waveguide components for frequencies of 3000 mc and 10,000 mc. While the radio frequency and VHF bridges are capable of measuring resistance and reactance directly, the lack of variable standard impedances for microwave bridges have largely limited them to comparison devices (Ref. 25). Thus an unknown impedance can be compared with a matched load by employing a "magic-tee" as the microwave bridge element. If a barretter or crystal rectifier detecting element is placed in the proper arm of the magic-tee the VSWR of the unknown load can be measured directly.

1.1.4 The MacPherson-Kerns Method. A precision method for measuring the complex reflection coefficient of an unknown load has recently been reported by MacPherson and Kerns (Ref. 41). The generator and detector are connected to two arms of a waveguide H-plane tee. Tuning elements in the junction are adjusted to provide a match looking into the third arm, to which the unknown is joined. The technique requires the use of a reflectionless variable phase device which is inserted between the junction and the unknown load, such as might be procured with a carefully designed line stretcher.

Motion of the phase shifter causes the standing-wave pattern to sweep past the fixed location of the detector, from which the amplitude and phase angle of the complex reflection coefficient of the movable load may be obtained. The probe and slot errors present in the slotted line are avoided by this arrangement, resulting in a precision microwave impedance measuring device. Furthermore, tight coupling between the detector and the waveguide junction is possible without severe distortion of the standing-wave pattern. Consequently, the relatively insensitive barretter detecting element can be used in place of the crystal rectifier leading to improved accuracy because of the former's superior response-law characteristic.



While the method is capable of precisely measuring small reflections, the large dynamic ranges to which the barretter would be subjected in the presence of loads having very large standing wave ratios tend to limit its usefulness.\* Also, the accuracy of the procedure is impaired if the phase-shifter produces variable reflections as the position of the load, with respect to the waveguide junction, is changed.

It is also apparent that an alternative procedure for producing a standing-wave pattern, which moves with respect to a fixed detector, may be accomplished by changing the frequency in some prearranged manner. This approach was examined during an early stage of the present investigation at this University, but has subsequently been discarded. In general, lossless tuning elements are quite sensitive to frequency changes. In addition, the unknown load may undergo rapid impedance changes for frequency variations occurring over certain ranges. Finally, probe distortion of the standing wave pattern in conventional slotted lines may become severe even for relatively small frequency changes (Ref. 13) owing to improper tuning.\*\*

1.1.5 The Double-Slug Transformer Method. Two dielectric slugs may be inserted in a transmission line for broad-band impedance matching. The lengths of the dielectric slugs are chosen to be one-quarter wavelength at the center frequency of the band. Their relative positions are then adjusted so that reflections from the slugs cancel load reflections.

This technique, which has been used in both waveguide and coaxial transmission lines, has been adapted for the measurement, as well as the matching, of load impedances (Ref. 20). The required information for computing the impedance consists of the length, spacing, position and "effective" dielectric constant of the slugs in addition to the wavelength. A procedure is available for the experimental determination of the effective dielectric constant.

---

\* However, from a study of the existing technique it appears that the procedure might easily be modified to accommodate a variable precision (waveguide) attenuator. This would allow the substitution principle to be employed for very precise large standing wave ratios.

\*\* It is assumed that a tuned probe would be employed.

It is asserted (Ref. 20) that this procedure possesses certain advantages over the conventional slotted line technique, owing to the fact that the only electrical measurement necessary is a suitable indication of a matched condition. A number of devices such as directional couplers, magic-tees, multi-arm bridges and multi-probe systems may be employed in conjunction with movable reflectionless loads to establish the matched condition. The absence of a slot and probe eliminate errors of the type present in slotted systems. It also appears that the procedure is less susceptible to the detrimental effects produced by mechanical imperfections than its slotted line counterpart.

Measurements of load VSWR between 2 and 7 were made (Ref. 20) over the frequency range of 700-1400 mc. The results are in good agreement with corresponding slotted line measurements of the same unknown loads.

The principal disadvantage in the method is the necessity for accurately measuring the "effective" dielectric constant of the slugs, since an error in its determination can lead to serious errors in the resulting impedance measurement. Another drawback is the necessity for fabricating a number of dielectric slugs.

1.1.6 The Reflectometer Method. The development of waveguide and coaxial directional couplers having a high directivity over a wide range of frequencies has led to still another method of measuring the complex reflection coefficient. The reflectometer (Ref. 45) consists basically of two directional couplers arranged in such a manner that the incident and reflected signals from an unknown load appear as separate outputs from the forward and reverse couplers, respectively. Generally, matched crystals must be employed for the detecting elements in order that their outputs may be directly compared by means of a ratio meter. A commercial version of this device, developed by the Hewlett-Packard Company, provides for visual display with swept frequency operation. Thus, load VSWR can be instantly examined over a given frequency band as some parameter is subjected to prescribed variations. Furthermore, a modification of the device also permits the determination of the phase angle of the load reflection coefficient so that microwave impedances may also be measured (Ref. 25).

Its accuracy is greatest at small values of load VSWR and decreases with increasing VSWR as a result of the larger dynamic range to which the detectors are subjected (Ref. 78). Although barretters may be preferable because of their superior response-law characteristics as compared to crystal rectifiers, the accuracy is nonetheless dependent upon how closely these barretters follow the desired law. A study made by Laskin (Ref. 40) indicates that commercial types of barretters may deviate from a square law response at the rate of 10 per cent per milliwatt. As mentioned above, reflectometers often require matched detecting elements when used in conjunction with other equipment. In addition, errors may also arise due to a departure of the forward and reverse couplers from the condition infinite directivity. When the ratio meter is used, the coupling does not have to be uniform over the frequency range under investigation, but it must vary in exactly the same manner in each directional coupler.

## 1.2 Standing Wave Ratio Measurement Techniques

1.2.1 The Direct Method. The simplest method for measuring standing wave ratio with a single movable probe in a slotted line is to use a detector of known response-law and to record the rectified current it delivers to a D'Arsonval type of indicating instrument. For example, if the rectified current is exactly proportional to the square of the voltage applied to the detector, over the entire dynamic range involved in the experimentation, then the voltage standing wave ratio is given by

$$\rho = \sqrt{\frac{I_{\max}}{I_{\min}}} \quad (7)$$

where

$I_{\max}$  = rectified current recorded at the standing wave maximum, and

$I_{\min}$  = rectified current recorded at the standing wave minimum.

In recent years commercial "standing wave indicators" have become available which provide a direct reading of standing wave ratio. This is accomplished by calibrating the scales of the indicator to read correctly when a square law device is used. The position of the standing wave maximum is found at which

the meter is set to zero. The detector is then moved to the location of the minimum at which point the indicator reads the standing wave ratio. In order to avoid the problems associated with drift in dc amplifiers the instrument employs a narrow band ac amplifier. The signal source is then switched on and off at the rate of 1000 cps. After detection this audio switching voltage is delivered to the ac amplifier of the standing wave indicator.

A serious disadvantage of the direct method of measuring standing wave ratio is that where very large values of VSWR are involved the detecting element must operate over a large portion of its characteristic. Under these conditions it is found that the deviation from square law response may be very great, leading to serious errors in the measured standing wave ratio. In spite of the fact that barretters are superior to crystal rectifiers in their ability to follow a square law response over wide dynamic ranges, they are less sensitive than crystals, thereby requiring larger source power for operation.

Experimental evidence suggests that the direct method of VSWR measurement cannot give precise results for ratios in excess of about 20:1.

1.2.2 The Small Reflection Method. As the VSWR of the unknown load decreases toward unity the accuracy of the direct method is again seriously reduced. This occurs because the small but finite reflections produced by the effects of the slot, probe and connectors become large in proportion to the unknown load.

There are several well known techniques for measuring the load VSWR in the case of small reflections (References 22, 25, 74). One of those most widely used was developed by Feenberg (Ref. 22). The load is made part of a coupling network which is terminated in a movable short circuit. The slotted line is placed between the source and the load. As the short circuit is moved through a series of known positions the location of the standing wave minima observed on the slotted line are measured relative to a suitably chosen reference plane. If the short circuit is continuously moved in a certain direction it is found that the location of the minima periodically oscillate about a median line. This behavior has been attributed to the constructive and destructive interference between the waves reflected from the short circuit and

those from the discontinuities in the (load) coupling network. The resulting curve and the associated reference planes may be used to obtain the magnitude and phase angle of the load reflection coefficient.

An alternative arrangement is obtained by replacing the slotted line with another movable short circuit, thus making the load part of a cavity (Ref. 25). One short circuit then has provisions for delivering energy from the source to the cavity while the other is arranged to deliver a small fraction of this energy to a detector. Either short circuit may be moved through a series of known positions while the other one is adjusted to give a resonant indication at each position. The information obtained is equivalent to that obtained with Feenberg's procedure, and the data is interpreted in a similar manner.

A third method makes use of a sliding, nearly reflectionless load (References 25, 74). A slotted line is connected between the signal source and the unknown whose VSWR is to be determined; the latter being terminated in the sliding load. The position of the probe and the sliding load are simultaneously adjusted to provide the highest obtainable VSWR as observed on a standing wave indicator. This will be designated as  $\rho_1$ .

A second VSWR measurement is made by first returning the probe to the position of the standing wave maximum as used in the preceding observation. With the detector held fixed at this position, the sliding load is adjusted for a minimum reading on the indicator. This second VSWR, which will be smaller than the first, is designated as  $\rho_2$ . The standing wave ratio of the unknown load is then given by (Ref. 74)

$$\rho = \frac{\rho_2 + 1}{\rho_2 - 1 + 2 \frac{\rho_2}{\rho_1}} \quad (8)$$

While this information yields only the magnitude of the load reflection coefficient, its phase angle may also be obtained through a proper choice of reference planes (Ref. 25).

1.2.3 The Roberts-von Hippel Method. In 1946 Roberts and von Hippel published the results of a study undertaken during World War II to accurately determine certain properties of dielectric substances (Ref. 52). This work led to a method of measuring large standing wave ratios by sampling only a small portion of the wave in the vicinity of the minimum. The VSWR relation is derived below in a manner similar to that of Barlow and Cullen (Ref. 6).

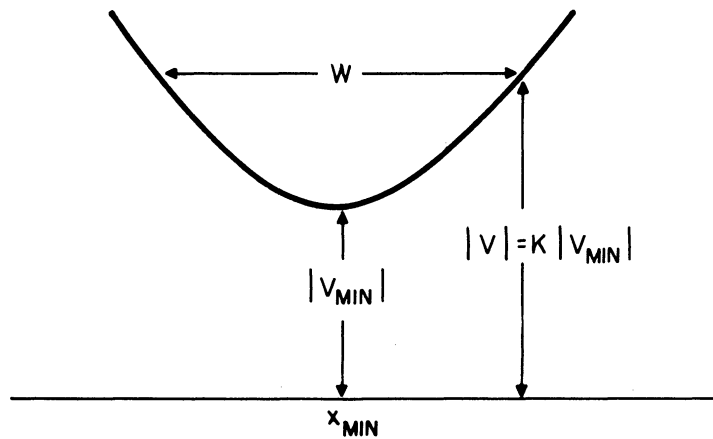


FIG. 1 CONDITIONS EXISTING NEAR A STANDING WAVE MINIMUM

Referring to Fig. 1, let it be assumed that  $|V_{\min}|$  represents the amplitude of the voltage at a standing wave minimum, located at the point  $x_{\min}$ , and let  $w$  be the distance between the points at which the amplitude of the voltage is  $K$  times its value at the minimum. If  $|V_i|$  represents the amplitude of the incident voltage, and if  $\Gamma_L$  is the load reflection coefficient, then provided the analysis is limited to a lossless transmission system having only one mode of propagation at a single frequency, it follows that

$$\left| \frac{V}{V_i} \right|^2 = 1 + |\Gamma_L|^2 - 2|\Gamma_L| \cos \beta w \quad . \quad (9)$$

At the position of the minimum the above relation becomes

$$\frac{|V_{\min}|^2}{|V_i|^2} = (1 - |\Gamma_L|)^2 \quad . \quad (10)$$

From Fig. 1, the expression for  $K^2$  may be obtained with the aid of the above two equations and a relation like (5),

$$K^2 = 1 + \frac{4|\Gamma_L|}{(1 - |\Gamma_L|)^2} \sin^2\left(\frac{\beta w}{2}\right) \quad . \quad (11)$$

Upon substituting equation (2) into (11) and solving for  $\rho$  there follows

$$\rho = \frac{1}{\sin\left(\frac{\beta w}{2}\right)} \sqrt{K^2 - \cos^2\left(\frac{\beta w}{2}\right)} \quad . \quad (12)$$

This is the Roberts-von Hippel relation. Large standing wave ratios can be measured through the application of this equation by accurately measuring the distance,  $w$ , between equal response points above the minimum using a precision dial gauge. Commercial gauges are available which have 0.001 millimeter graduations over a linear displacement range of 250 millimeters.

It will be evident from the foregoing analysis that the principal weakness of this method lies in the dependence which must be placed upon the detector response-law\* that determines the factor  $K$ . Not only must  $K$  be known but it also must be assumed to be constant over the portion of the standing wave used in the measurement. The dynamic range can be reduced by using small values of  $w$ , but this may lead to significant errors as a result of relatively small uncertainties in  $w$ . Alternatively, large values of  $w$  may be used if a barretter is used as the detecting element instead of a crystal rectifier. The sensitivity is much less for a barretter than for a crystal, however, so that it may be necessary to use much larger source power when employing it. In addition, the deviation from the square law characteristic

---

\* The same limitation is also imposed upon the resonance-curve impedance measurement procedure described in section 1.1.2.

of 10 per cent milliwatt for a barretter (Ref. 40) must be taken into consideration when using this procedure.

1.2.4 The Shunt Method. It is a well known fact that the highest VSWR which can be observed in any transmission system is limited by the residual losses of the system (Ref. 40). Recently, Oliner and Altschuler have applied this principle to the VSWR measurement of low loss dielectric materials (Ref. 47). The procedure requires a suitable lossy structure of known dissipation to be placed in shunt with a transmission line containing the dielectric. Through the use of good design techniques and careful silver plating it is possible to construct a transmission system having negligible loss compared to the dielectric being studied. Even if this condition is not realized separate measurements may be made on the transmission system to determine its dissipation.

Standing wave measurements are then carried out on the composite system containing the dielectric sample and the lossy shunt network. The proper selection of the shunt network permits the observed VSWR to be reduced enough so that accurate methods for small standing wave ratios may be used in the measurement. The knowledge of the loss characteristics of the shunt network then permits the VSWR of the dielectric to be obtained computationally. It is interesting to observe that the authors were able to measure a dielectric whose VSWR in the microwave frequency range was\* 61.6 from an observed VSWR of less than 20. The chief disadvantage appears to be the necessity of determining the loss characteristics of the shunting structure.

1.2.5 The Winzemer Method. In 1950 Aaron Winzemer (Ref. 77) published the results of a study conducted at the Naval Research Laboratory pertaining to an improved method of measuring voltage standing wave ratio. Starting with the basic relations for a lossless transmission line and using general expressions for the detector response-law, he derived the equation

---

\* Actually, due to measurement uncertainties the authors give the result

	+4.3
61.6	
	-3.7



for the voltage standing wave ratio in terms of electrical angles measured on the line. This significant development led to a technique for VSWR measurement which does not depend upon the detector response-law. The method was also extended to include transmission lines with finite losses. In addition, a number of special cases were treated leading to VSWR relations which may be conveniently applied to various portions of the standing wave.

The technique has been subjected to intensive study at this University and measurements made by Winzemer's procedure have been compared to the method developed here. Since accurate measurement of electrical angles (or linear displacements) on the line is the only important requirement, the procedure may be employed with the usual slotted line to which a precision dial gauge is attached.

Experience thus gained with the technique has indicated that, under certain circumstances, an important source of error may arise. In spite of the fact that the general response law of a given detector does not have to be known in this method, it is necessary to assume that the tuning of the probe remains unchanged regardless of its location along the slotted line. When large segments of the standing wave are explored any physical conditions which lead to a variation in the probe tuning can often cause significant distortion of the pattern, due to the effects of non-zero probe susceptance (References 4, 13, 65).

When sufficient signal strength is available to permit the use of barretters as detecting elements these troublesome effects are not present. However, when limited source power requires the use of the more sensitive crystal rectifiers, experimental evidence tends to indicate that pattern distortion may be very serious. The explanation appears to be associated with the characteristics of the non-linear barrier layer capacity.\* After the

---

\* See for example, Crystal Rectifiers (MIT Radiation Laboratory Series, Vol. 15), Torrey and Whitmer, McGraw-Hill Book Co., Inc., New York, 1948.

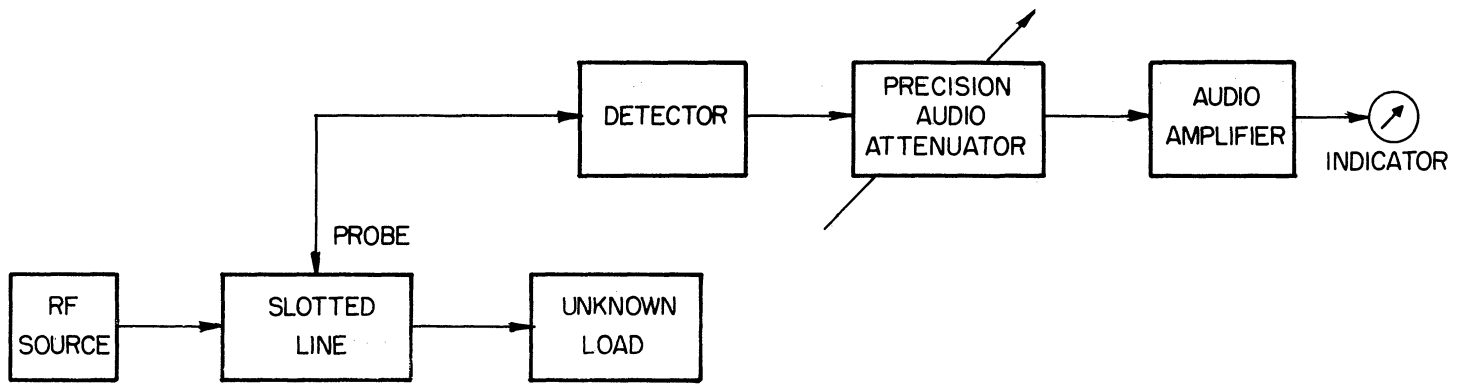
detector has been properly tuned, as explained subsequently in connection with the measurement procedure, the probe is then moved to selected points on the standing wave from which electrical angular data is obtained. The different standing wave voltages at these various points may produce sufficient changes in the barrier layer capacity of the crystal rectifier to result in severe mis-tuning of the detector with accompanying pattern distortion.

Independent measurements described later tend to confirm this explanation. It has also been found that the validity of the probe tuning procedure depends upon the dynamic range to which the detector is subjected.

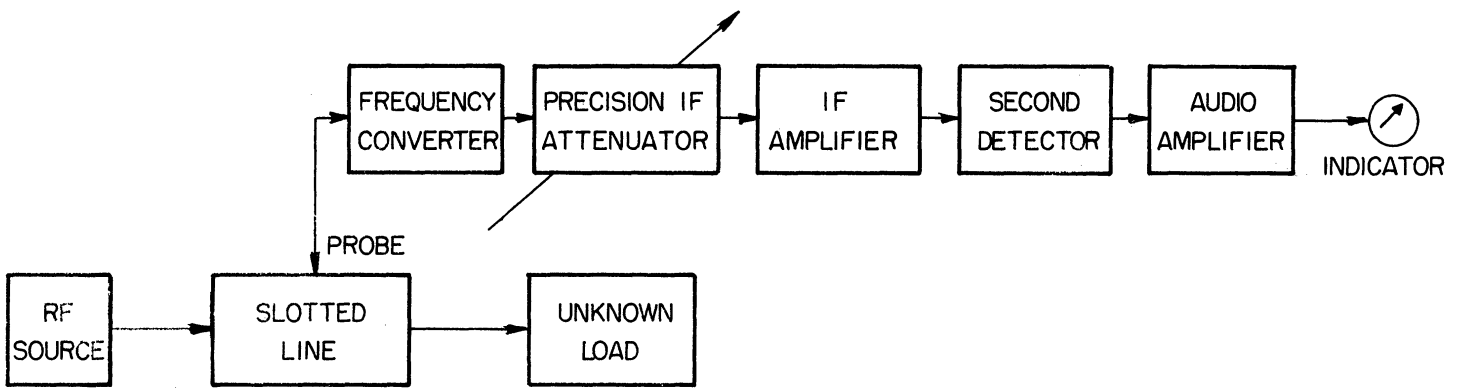
1.2.6 The Substitution Method. It has been pointed out in the discussion of several of the VSWR measurement procedures described previously that the detector characteristics may seriously affect the accuracy of standing wave measurements over large amplitude ranges. To circumvent this limitation, several substitution or "slide-back" procedures may be used for the measurement of large standing wave ratios, which are capable of providing a higher degree of measurement accuracy than those discussed above.

The substitution technique was originally applied to precision microwave attenuation measurements (References 25, 38, 39, 45, 51, 78). Three basic versions may be employed, depending upon the frequency at which the variable standard attenuator is incorporated into the measurement. As described in connection with the direct method of measuring VSWR, the signal source is 100 per cent square wave modulated at the rate of 1000 cps. While this feature is not strictly required for the IF substitution procedure, it may readily be applied to any of the methods indicated in Fig. 2.

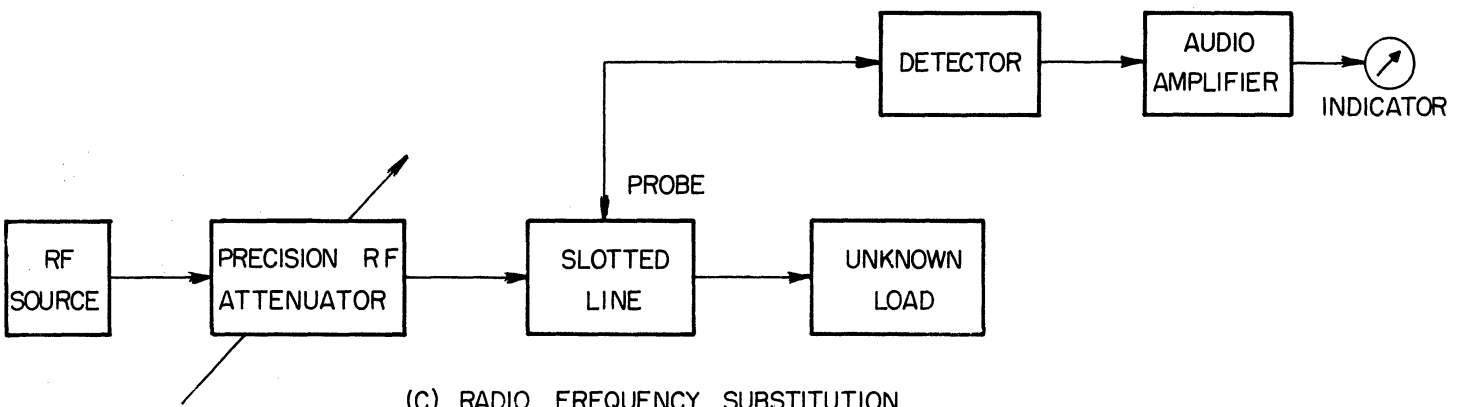
The audio substitution procedure utilizes a slotted line which is terminated in the unknown load whose VSWR is to be determined. A probe, which samples the electric field in the transmission system, delivers energy to a barretter or crystal rectifier detecting element. The detector, with its associated rf filter, extracts the 1000 cps square wave envelope from the microwave signal and delivers it, through a variable precision audio attenuator, to an audio amplifier for display on the indicator. The measurement is performed by first locating the probe at a convenient standing wave minimum.



(A) AUDIO FREQUENCY SUBSTITUTION



(B) INTERMEDIATE FREQUENCY SUBSTITUTION



(C) RADIO FREQUENCY SUBSTITUTION

FIG.2 SUBSTITUTION METHODS FOR MEASURING STANDING WAVE RATIO

The variable precision attenuator is adjusted to provide a suitable reading on the indicator. The probe is then moved to a standing wave maximum. The setting of the attenuator is now increased to provide the same indicator reading as previously. The difference in the two attenuator readings is the VSWR of the unknown load expressed in decibels.

A study of the audio substitution method of measuring VSWR reveals that, while the measurement accuracy is not limited by the characteristics of the amplifier and indicator, since they operate at fixed levels, the barretter response-law has an important bearing on the ultimate precision. In spite of this restriction, Korewick (Ref. 38) reported on a similar system for measuring attenuation which yields accurate results to within 0.1 db over a dynamic range of 40 db. The available dynamic range is largely determined by noise and the detector response-law characteristics.

In the intermediate frequency substitution method the probe delivers energy to a frequency converter which generates the required IF signal. A variable precision attenuator adjusts the level of the signal reaching the IF amplifier, second detector, audio amplifier and indicator. Just as with the audio frequency substitution procedure, the measurement is carried out by setting the precision IF attenuator for a convenient level on the indicator when the probe is at a standing wave minimum. The probe is moved to a standing wave maximum and the attenuation is increased to return the indicator to its original reading. The difference in the two values of attenuation yields the standing wave ratio.

Systems of this type for measuring attenuation have been developed by Gainsborough (Ref. 24) and by Grantham and Freeman (Ref. 29). Very high measurement accuracy can be obtained, leading to uncertainties of only 0.2 per cent. A dynamic range of 50 db has been realized. The use of a super-heterodyne receiver provides such high sensitivity that the probe can be very loosely coupled to the transmission system. If the local oscillator signal is strong compared to the rf signal, the frequency converter produces an intermediate frequency signal which is linearly proportional to the rf signal in the slotted line. Standing wave ratios as high as 10,000 have been claimed with this technique (Ref. 78).

Though generally small, the principal sources of error in the IF substitution procedure arise as a result of the departure of the frequency converter (which is usually a crystal rectifier) from linearity. In addition, the frequency and power level stability of the local oscillator and its subsequent effect upon the behavior of the converter become important factors when high precision is involved.

The rf substitution procedure employs a variable precision attenuator located between the signal source and the slotted line. As in the foregoing methods, the attenuator is adjusted to give the same reading when the probe is located at a standing wave maximum as it has at a standing wave minimum. The difference in attenuator readings is equal to the VSWR expressed in decibels. The most important characteristic of this procedure is the fact that the accuracy of the resulting measurement depends primarily on the nature of the precision attenuator. In waveguide systems, variable precision attenuators having a small minimum attenuation and a very low VSWR over wide frequency ranges are commercially available. The only variable precision attenuators presently in use in coaxial systems, on the other hand, are those of the waveguide below cutoff types (Ref. 51). Their high minimum attenuation requires the use of a signal generator having a larger power output than the audio frequency and intermediate frequency substitution methods. If a specially designed probe were constructed (without the usual provisions for a barretter or crystal rectifier), its output could be delivered to a high sensitivity microwave receiver to permit the rf substitution procedure to be used with low power signal generators.

It is interesting to observe that while the rf substitution method using a precision attenuator can be employed for measuring VSWR, Vogelman (Ref. 69) used standing wave measurements for the accurate determination of very small values of attenuation. The VSWR measurement was performed using a variable precision waveguide attenuator that had been accurately calibrated at the 0 and 3 db points.

A modification of the rf substitution procedure using a commercial fixed precision coaxial attenuator has been developed at this University. The theoretical background is presented in the next chapter and the measurement technique is explained in the third chapter. An analysis of the sources of error is presented in the last chapter.

## 2. DERIVATION OF THE GENERAL RELATIONS

The general equations which relate the electrical angles on the transmission line to the voltage standing wave ratio are obtained from a study of the vectors used to represent the incident, reflected and total voltages in the system. The most important restrictions placed on this analysis are that the system is lossless and only one of the possible propagating modes exists. Under these conditions the amplitudes of the incident and reflected voltages are constant at any point along the line. Since the reflection coefficient for the coaxial line will be taken as the ratio of the reflected voltage to the incident voltage at any point, its amplitude will likewise be constant all along the line.\*

It will also be assumed that the source generates a signal whose frequency and maximum amplitude are time invariant, and that the rf fields vary sinusoidally in time and space. The load may have any arbitrary impedance value; however, it will generally be assumed to be composed of passive circuit elements. The entire system, consisting of the transmission line, source and load, will be assumed linear so that the superposition principle may be applied. The detector response-law will not be considered since the rf substitution method of measuring VSWR removes any dependence on the detector characteristics.\*\* Moreover, all precision fixed coaxial attenuators which are used in the measurement procedure will be assumed to be linear, passive, bilateral networks of known attenuation.

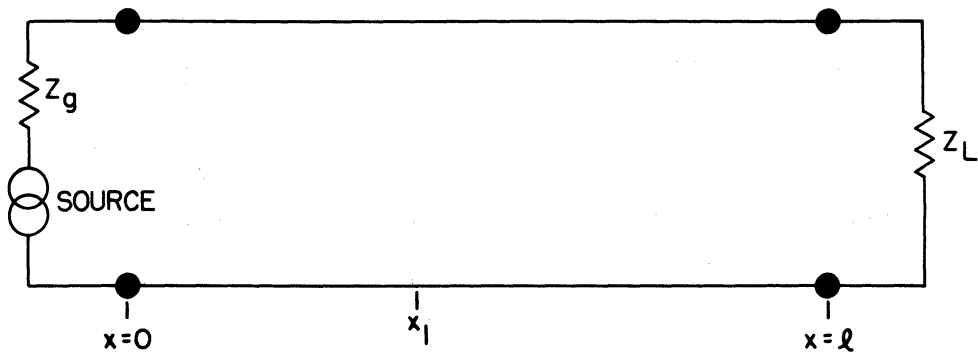
### 2.1 The Vector Relations in Lossless Systems

The foregoing assumptions make it possible to represent the transmission system, whether it be a coaxial line or a waveguide, as the parallel wire pair of Fig. 3.

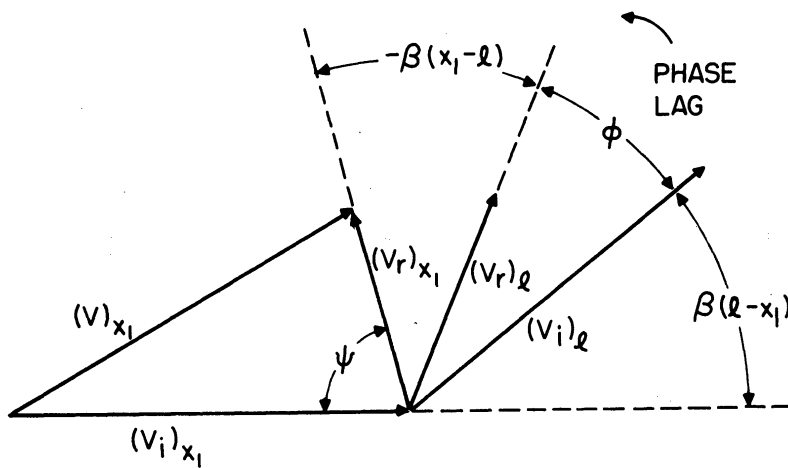
---

\* In waveguide systems, the corresponding reflection coefficient is defined as the ratio of the reflected electric field (in a transverse plane) to the incident electric field (in the same transverse plane) at any point along the guide.

\*\* The material presented in this chapter also applies to the IF substitution procedure to the extent that the frequency converter can be considered linear.



(a) The Transmission Line Equivalent Circuit



(b) The Vector Relations

FIG. 3 THE REPRESENTATION OF LOSSLESS TRANSMISSION SYSTEMS

The uniform characteristic impedance of the line in this single propagating mode is designated by  $Z_0$ , and the source impedance by  $Z_g$ . The load reflection coefficient has a magnitude  $|\Gamma_L|$  and a phase angle  $\phi$ . The x-coordinate, which represents the one dimensional space variable, increases positively in the direction of the load.

The point  $x_1$  will be chosen for a study of the vector relations. The incident voltage amplitude at  $x_1$ , namely  $|V_i|_{x_1}$ , is situated in the horizontal position. The incident and reflected voltage amplitudes at  $l$  are indicated as  $|V_i|_l$  and  $|V_r|_l$ , respectively, and the reflected voltage amplitude at  $x_1$  is designated as  $|V_r|_{x_1}$ . The angle  $\psi$  shown in Fig. 3(b) is equal to

$$\psi = 180 - 2\beta(l - x_1 + \frac{\phi}{2\beta}) \text{ degrees.} \quad (13)$$

Clearly,  $\psi$  depends upon the length of the transmission line, the location of  $x_1$  and the phase angle of the load reflection coefficient. In the work that follows it becomes convenient to consider that all measurements are made relative to either a standing wave maximum or a standing wave minimum. Upon employing this translation it follows that  $x = 0$  at either a maximum or minimum and  $x_1$  now represents the displacement from this maximum or minimum. Since the line is lossless the magnitude of the reflection coefficient at any value of  $x$  is constant, and there are then two special cases as shown in Fig. 4.

The familiar trigonometric relations yield

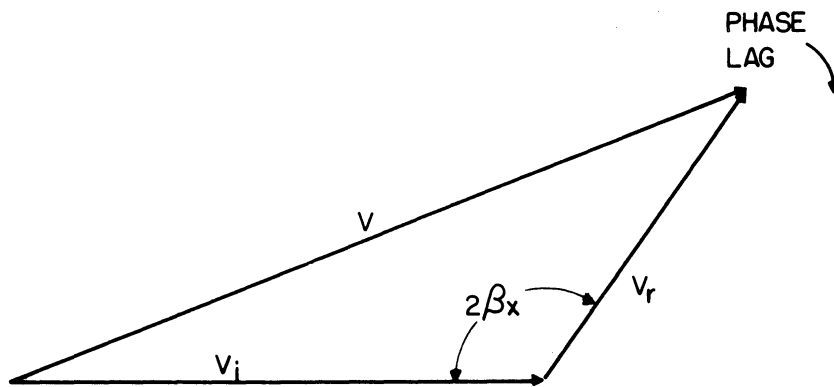
$$\left| \frac{V}{V_i} \right|^2 = 1 + |\Gamma|^2 \pm 2|\Gamma| \cos 2\beta x, \quad (14)$$

the positive sign associated with the third term of the right member applying to Fig. 4(b), and the negative sign applying to Fig. 4(a).

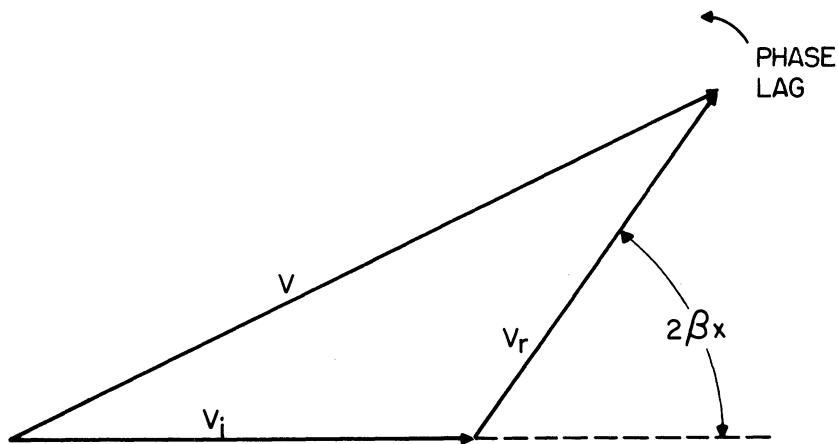
## 2.2 Selection of Coordinate Reference

2.2.1 The Standing Wave Maximum. As a matter of convenience the following definitions are made





(a) Vector Relations at Point  $x$  Measured From a Standing Wave Minimum



(b) Vector Relations at Point  $x$  Measured From a Standing Wave Maximum

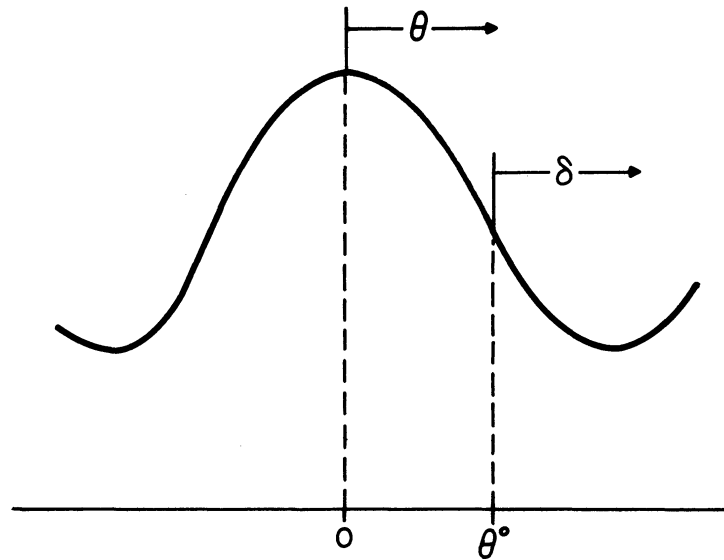
$$|V_r| = |\Gamma| |V_i|$$

FIG. 4 VECTOR RELATIONS FOR A STANDING WAVE MAXIMUM AND MINIMUM

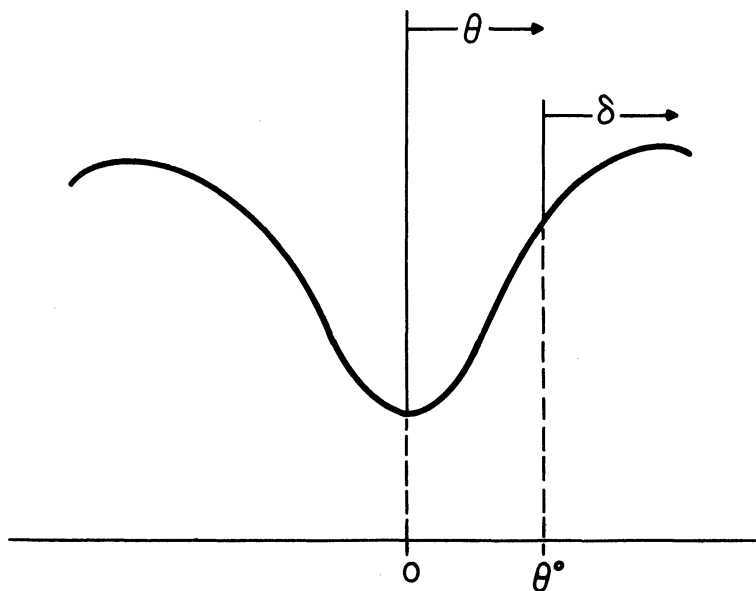
$$\theta \triangleq \beta x \quad , \quad (15)$$

$$\theta \triangleq \theta_0 + \delta \quad , \quad (16)$$

these angles being positive when measured in the direction indicated (by arrows) in Fig. 5 (a).



(a) The Standing Wave Maximum as the Coordinate Reference



(b) The Standing Wave Minimum as the Coordinate Reference

FIG. 5 DEFINITION OF THE ELECTRICAL ANGLES

Upon substituting equation (15) into (14) the right member can be normalized to unity at the angle  $\theta_0$ , which is measured relative to a standing wave maximum, provided

$$\left| \frac{V}{V_i} \right|_{\text{unity at } \theta_0}^2 = \frac{1 + |\Gamma|^2 + 2|\Gamma| \cos 2\theta}{1 + |\Gamma|^2 + 2|\Gamma| \cos 2\theta_0} \quad (17)$$

Equation (2), together with a relation like (5), may be used in conjunction with (17) to obtain

$$\left| \frac{V}{V_i} \right|_{\text{unity at } \theta_0} = \sqrt{1 + \frac{(\rho^2 - 1)(\sin^2 \theta_0 - \sin^2 \theta)}{\rho^2 - (\rho^2 - 1)\sin^2 \theta_0}} \quad (18)$$

It is convenient to define the quantity  $\alpha$  according to the relation

$$\alpha \triangleq 20 \log_{10} \left| \frac{V}{V_i} \right|_{\text{unity at } \theta_0} \text{ decibels.} \quad (19)$$

Thus,  $\alpha$  is either zero or a negative number because the voltage magnitude at any point on the standing wave pattern cannot exceed the voltage magnitude at the maximum. If equation (18) is now applied to (19) the standing wave ratio is found, with the aid of (16), to be

$$\rho = \sqrt{\frac{\sin^2(\theta_0 + \delta) - 10^{\frac{\alpha}{10}} \sin^2 \theta_0}{10^{\frac{\alpha}{10}} \cos^2 \theta_0 - \cos^2(\theta_0 + \delta)}} \quad (20)$$

The result expressed by equation (20) is the first of the general relations which shows that the voltage standing wave ratio depends only upon the value of  $\alpha$  and the angles  $\theta_0$  and  $\delta$ . The origin of the coordinate system, from which  $\theta_0$  is measured, is the location of the standing wave maximum. The angle  $\delta$  is then measured relative to  $\theta_0$ .

2.2.2 The Standing Wave Minimum. From a study of Fig. 5 (b), it may be observed that  $\theta_0$  and  $\delta$  can be defined in relation to a standing wave minimum just as they previously were relative to a standing wave maximum. Accordingly, equations (15) and (16) apply here with  $\theta$  or  $x$  being zero at the minimum.

Following a line of development similar to that used in the derivation of equation (20) it is found that

$$\rho = \sqrt{\frac{\frac{\alpha}{10} \cos^2 \theta_0 - \cos^2(\theta_0 + \delta)}{\sin^2(\theta_0 + \delta) - 10^{-10} \sin^2 \theta_0}} \quad (21)$$

Alternatively, equation (21) can be obtained directly from (20) by considering the references from which  $\theta_0$  is defined in the two cases. The result expressed by equation (21) is the second of the general relations. Again, it may be observed that the standing wave ratio depends only upon  $\alpha$ ,  $\theta_0$  and  $\delta$ . However, in the present case  $\alpha$  is either zero or positive and  $\theta_0$  is measured in relation to a standing wave minimum. The angle  $\delta$  is measured relative to  $\theta_0$ , as before.

### 2.3 Table of Standing Wave Relations

The general relations lead to an infinite set of expressions which can be used, in principle at least, for the measurement of standing wave ratio at any point on the wave. The special forms which they assume for several important angles are specified in Table I.

Since the angular increments of  $\theta_0$  when applied to equation (20) yield the same results as the application of  $(\theta_0 - 90^\circ)$  to equation (21), one table suffices. While the angle  $\delta$  is always measured relative to  $\theta_0$  regardless of whether the standing wave maximum or minimum is used for the coordinate reference, somewhat greater care must be exercised in the interpretation of the quantity  $\alpha$ . When the maximum is the coordinate reference and  $\theta_0 = 0$ ,  $\alpha$  is either zero or negative; when  $\theta_0 = 90^\circ$ ,  $\alpha$  is either zero or positive. When the minimum is the coordinate reference and  $\theta_0 = 0$ ,  $\alpha$  is either zero or

TABLE I

## THE STANDING WAVE RELATIONS

$\theta_0$ Measured From Maximum (Eq. 20)	The Standing Wave Relation	$\theta_0$ Measured From Minimum (Eq. 21)
$0^\circ$	$\rho = \frac{\sin \delta}{\sqrt{10^{\alpha/10} - \cos^2 \delta}}$	$-90^\circ$
$30^\circ$	$\rho = \sqrt{\frac{\sqrt{3} \sin 2\delta + 2 \sin^2 \delta + 1 - 10^{\alpha/10}}{\sqrt{3} \sin 2\delta - 2 \cos^2 \delta - 1 + 10^{\alpha/10}}}$	$-60^\circ$
$45^\circ$	$\rho = \sqrt{\frac{\sin 2\delta + 1 - 10^{\alpha/10}}{\sin 2\delta - 1 + 10^{\alpha/10}}}$	$-45^\circ$
$60^\circ$	$\rho = \sqrt{\frac{\sqrt{3} \sin 2\delta + 2 \cos^2 \delta + 1 - 10^{\alpha/10}}{\sqrt{3} \sin 2\delta - 2 \sin^2 \delta - 1 + 10^{\alpha/10}}}$	$-30^\circ$
$90^\circ$	$\rho = \frac{1}{\sin \delta} \sqrt{10^{\alpha/10} - \cos^2 \delta}$	$0^\circ$
$120^\circ$	$\rho = \sqrt{\frac{\sqrt{3} \sin 2\delta - 2 \cos^2 \delta - 1 + 10^{\alpha/10}}{\sqrt{3} \sin 2\delta + 2 \sin^2 \delta + 1 - 10^{\alpha/10}}}$	$30^\circ$
$135^\circ$	$\rho = \sqrt{\frac{\sin 2\delta - 1 + 10^{\alpha/10}}{\sin 2\delta + 1 - 10^{\alpha/10}}}$	$45^\circ$
$150^\circ$	$\rho = \sqrt{\frac{\sqrt{3} \sin 2\delta - 2 \sin^2 \delta - 1 + 10^{\alpha/10}}{\sqrt{3} \sin 2\delta + 2 \cos^2 \delta + 1 - 10^{\alpha/10}}}$	$60^\circ$
$180^\circ$	$\rho = \frac{\sin \delta}{\sqrt{10^{\alpha/10} - \cos^2 \delta}}$	$90^\circ$

positive; when  $\theta_0 = 90^\circ$ ,  $\alpha$  is either zero or negative. For other values of the angle  $\theta_0$ ,  $\alpha$  may be either positive or negative since standing wave amplitudes both larger and smaller than those found at  $\theta_0$  exist.

#### 2.4 An Important Special Case

Although the foregoing analysis shows that an infinite number of relations exist, any one of which may be applied at an appropriate point on the wave, only the one corresponding to  $\theta_0 = 0$  in equation (21) has been studied extensively at this University. A set of curves have been plotted for

$$\rho = \frac{1}{\sin\delta} \sqrt{10^{\frac{\alpha}{10}} - \cos^2\delta}, \quad (22)$$

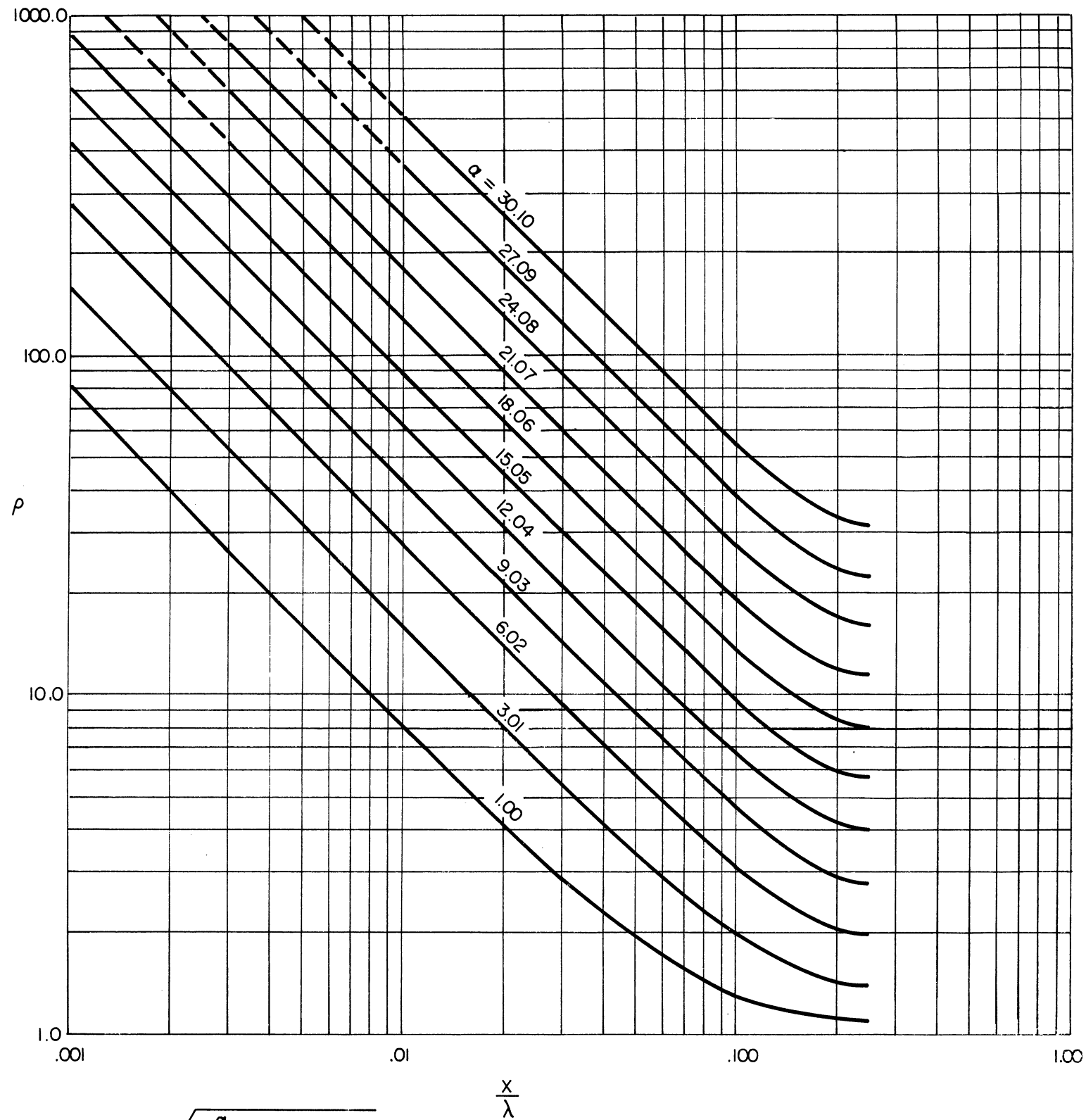
as a function of  $x/\lambda$  on log-log paper, Fig. 6. The choice of independent variable was influenced by the fact that

$$\delta = 2\pi(x/\lambda) \quad (23)$$

where  $x$  is the distance from the minimum to any point on the wave. The quantity  $\alpha$ , which represents a precisely known attenuation in the experimental procedure, is selected as a parameter. The curves are found to be nearly parallel straight lines over the ranges of greatest importance.

It may be observed that near their lower extremity considerable curvature exists. Thus, the curves asymptotically approach horizontal straight lines for very small values of VSWR. The physical significance of this behavior lies in the fact that there is a lower limit to the standing wave ratio which a given fixed precision attenuator can measure. If, for example, the attenuation is decibels is greater than

$$20 \log_{10} \frac{|V_{\max}|}{|V_{\min}|}$$



$$\rho = \frac{1}{\sin(2\pi x/\lambda)} \sqrt{10 \frac{a}{10} - \cos^2(2\pi x/\lambda)}$$

**FIG. 6**  
**VOLTAGE STANDING WAVE RATIO**  
**VS.**

**NORMALIZED DISPLACEMENT FROM THE POSITION OF THE MINIMUM**

where,

$$\begin{aligned} |V_{\max}| &= \text{magnitude of the voltage at a standing wave maximum, and} \\ |V_{\min}| &= \text{magnitude of the voltage at a standing wave minimum,} \end{aligned}$$

then that attenuator cannot be used to measure the VSWR of the wave. This is not a serious limitation, however, because fixed precision attenuators of 3 db are commercially available, which corresponds to a VSWR of 1.41:1. For smaller standing wave ratios the direct method employing a barretter as a detecting element is feasible for accurate measurements. Moreover, there appears to be no reason to believe that smaller precision attenuator values could not be manufactured.

The relation expressed by equation (22) is also interesting because of its similarity to the results of Chipman, equation (6), and of Roberts-von Hippel, equation (12). Thus, K in Chipman's equation and  $K^2$  in the Roberts-von Hippel equation correspond to  $10^{\alpha/10}$  in equation (22). The comparison must be applied with care, however, because  $\alpha$  is a linear quantity which does not depend upon the voltages to which it may be subjected; the constants K and  $K^2$ , on the other hand, are influenced by the detector characteristics and may be affected by the magnitude of the voltages applied to the crystal rectifier or barretter.

In the special case where  $\alpha = 3.01$  db, equation (22) becomes

$$\rho = \frac{1}{\sin\delta} \sqrt{2 - \cos^2\delta} \quad . \quad (24)$$

For large values of VSWR, the electrical angle  $\delta$ , measured between the standing wave minimum and the point 3.01 db above the minimum, becomes very small. The cosine function can then be replaced by unity and the sine function by its argument, leading to

$$\rho \approx \frac{\lambda}{\pi d} \quad , \quad (25)$$

where d is the distance between the points at which the power is twice the minimum power. This result, which can also be obtained from equations (6)



and (12), has been widely referred to as a useful approximation for the measurement of large standing wave ratios (References 25, 45, 73).

### 2.5 Relation Between VSWR, Wavelength and Twice Power Points

Inasmuch as several of the procedures used for measuring large standing wave ratios require the exploration of the pattern in the vicinity of the minimum, it is of interest to study the manner in which the distance  $d$ , between the twice minimum power points, changes with VSWR and with the operating wavelength.

Referring to equation (24), the distance  $x$  is first replaced by  $x_0$ , where the latter is the distance from the minimum to the point on the wave where the power is twice the minimum value. Assuming that the pattern is symmetrical in the region of the minimum, it then follows that  $x_0$  can be replaced by  $d/2$ , and the result, upon solving for  $d/\lambda$ , becomes\*

$$\frac{d}{\lambda} = \frac{1}{\pi} \sin^{-1} \frac{1}{\sqrt{\rho^2 - 1}} \quad (26)$$

A plot of this expression is given in Fig. 7, where it may be seen that  $d/\lambda$  is a straight line function of  $\rho$  (on log-log paper) for standing wave ratios in excess of 3:1. For large values of VSWR, equation (26) becomes identical to (25) and the resulting expression is recognized as the relation for an equilateral hyperbola (in rectangular coordinates), assuming that  $d/\lambda$  and  $\rho$  are the variables. Thus, as  $\rho$  increases beyond bound  $d/\lambda$  asymptotically approaches zero. However, the singular point at  $\rho = 1$  in equation (26) causes the curve to depart from the hyperbolic variation for small standing wave ratios.

The curve shows that for a standing wave ratio of 100:1 and a wavelength of ten centimeters the dimension  $d$  between twice minimum power points

---

\* It is clear from the nature of the derivation that this relation describes a physical behavior which exists regardless of the measurement procedure used.

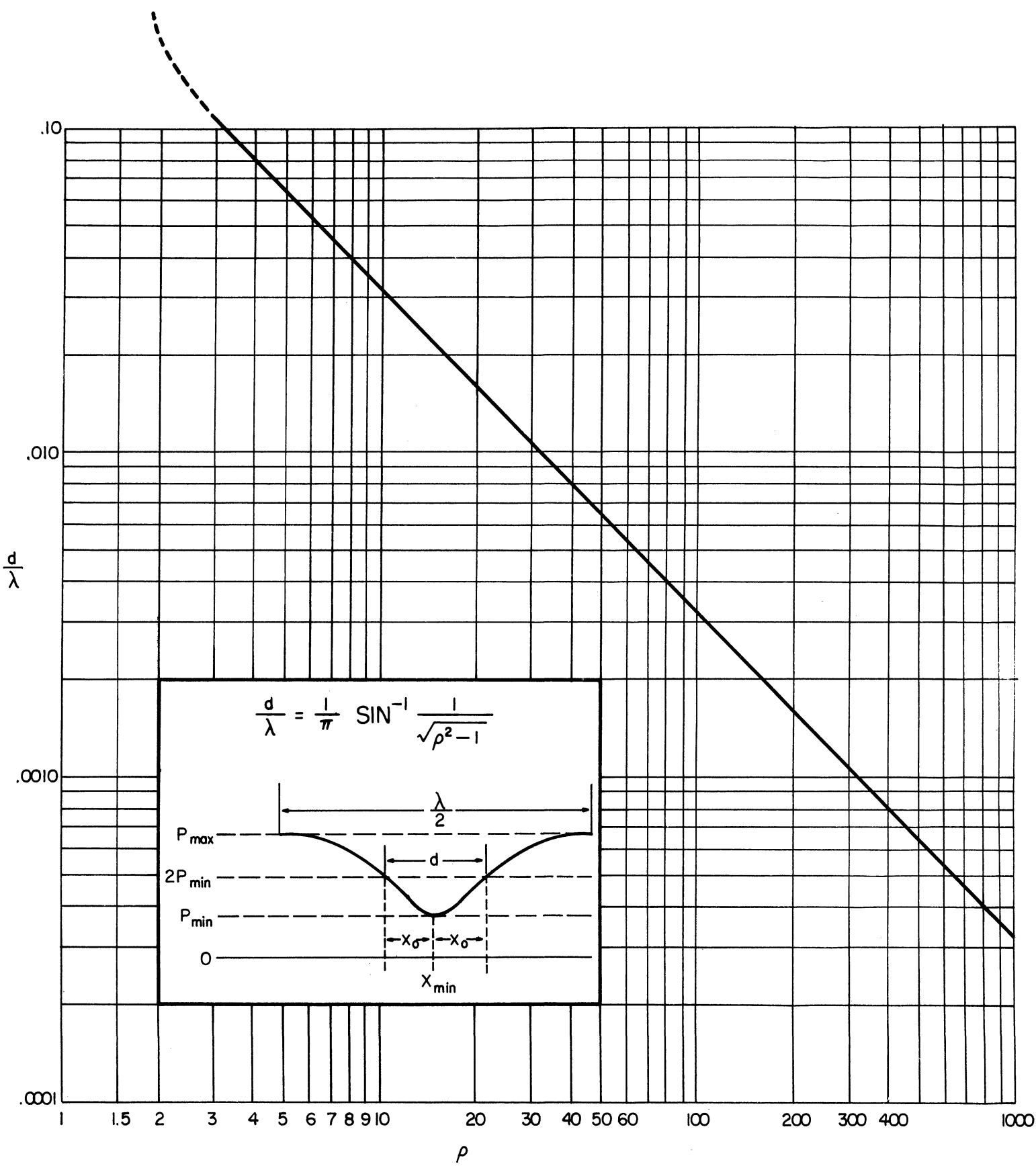


FIG. 7 RELATION BETWEEN VSWR, WAVELENGTH & TWICE POWER POINTS

is approximately 0.0126 inches. Since the diameter of the probe used on the slotted line at this laboratory is 0.060 inches, it is apparent that the signal level at the standing wave minimum is not being sampled. The indicator reading represents some sort of average value of the fields intercepted by the probe.

While it might at first appear that this behavior imposes a serious limitation on those methods of standing wave measurement which depend upon sampling the minimum field intensity, experimental evidence does not support this conclusion. Numerous observations were made on a load having a standing wave ratio of about 40:1 with several probes,\* the smallest of which is 0.0059 inches in diameter and the largest 0.060 inches in diameter. The observed standing wave ratio was found to be independent of the probe diameter, in spite of the fact that the dimension  $d$  is only 0.0315 inches for a wavelength of ten centimeters.

It is the author's belief that the explanation is associated with the shape of the standing wave pattern in the vicinity of the minimum. Thus, a standing wave ratio of 40:1 corresponds to a reflection coefficient magnitude of about 0.95. Barlow and Cullen (Ref. 6) show that the pattern varies almost linearly with  $x$  for reflection coefficient magnitudes larger than about 0.80. It would appear, then, that when large standing wave ratios are encountered an exact knowledge of the signal level at the minimum is not required. It is only necessary to know accurately the range of the linear portion of the curve which has been used in the measurement. In the rf substitution procedure, this information is easily obtained from the precision attenuator.

On the other hand, a standing wave ratio of only 10:1 corresponds to a reflection coefficient magnitude of about 0.82. While the curves of Barlow and Cullen show some slight evidence of curvature in the vicinity of the minimum, the dimension  $d$  is found to be 0.126 inches for a ten centimeter

---

\* A more complete description of this investigation is given in the last chapter.

wavelength. This is more than twice as large as the 0.060 inch diameter probe so that it becomes easier to determine the signal level at the minimum. For smaller standing wave ratios the pattern shows considerable curvature near the minimum (Ref. 6), but the dimension  $d$  is sufficiently large to permit an accurate sampling of the minimum field intensity.

While this fortuitous circumstance shows that the standing wave minimum does not have to be accurately known in order to measure large values of VSWR, it seems appropriate to recognize the existence of those physical conditions to which the probe may be subjected.

### 3. THE MEASUREMENT PROCEDURE

It was previously mentioned that, of the infinite number of possible relations which might be employed in the determination of standing wave ratio, only the minimum relation has been applied to measurements performed at this University. This is not necessarily to be construed as meaning that some or all of the remaining possible relations possess no practical value insofar as their incorporation into a measurement technique is concerned, but only that they have not been subjected to intensive study. Indeed, it may well be that one or more of the alternative procedures are superior to the minimum method for a variety of practical reasons. On the other hand, certain inherent disadvantages present in these other methods might severely detract from their potential utility. The resolution of these issues appears to be appropriately suited to a subsequent investigation.

Accordingly, the details of the procedure to be described should not be considered as the sole process by which the rf substitution procedure can be applied to the measurement of standing wave ratio. Rather, it should be regarded as a technique which yields accurate results over the range of measurements evaluated. Due to certain limitations imposed by existing laboratory facilities, the highest VSWR at which the procedure can give precise results is not presently known. It appears to be substantially higher than the largest values reported.

#### 3.1 The Matching Technique

The general arrangement of the test equipment employed in the present measurement procedure is shown in Fig. 8. The rf source consists of a standard

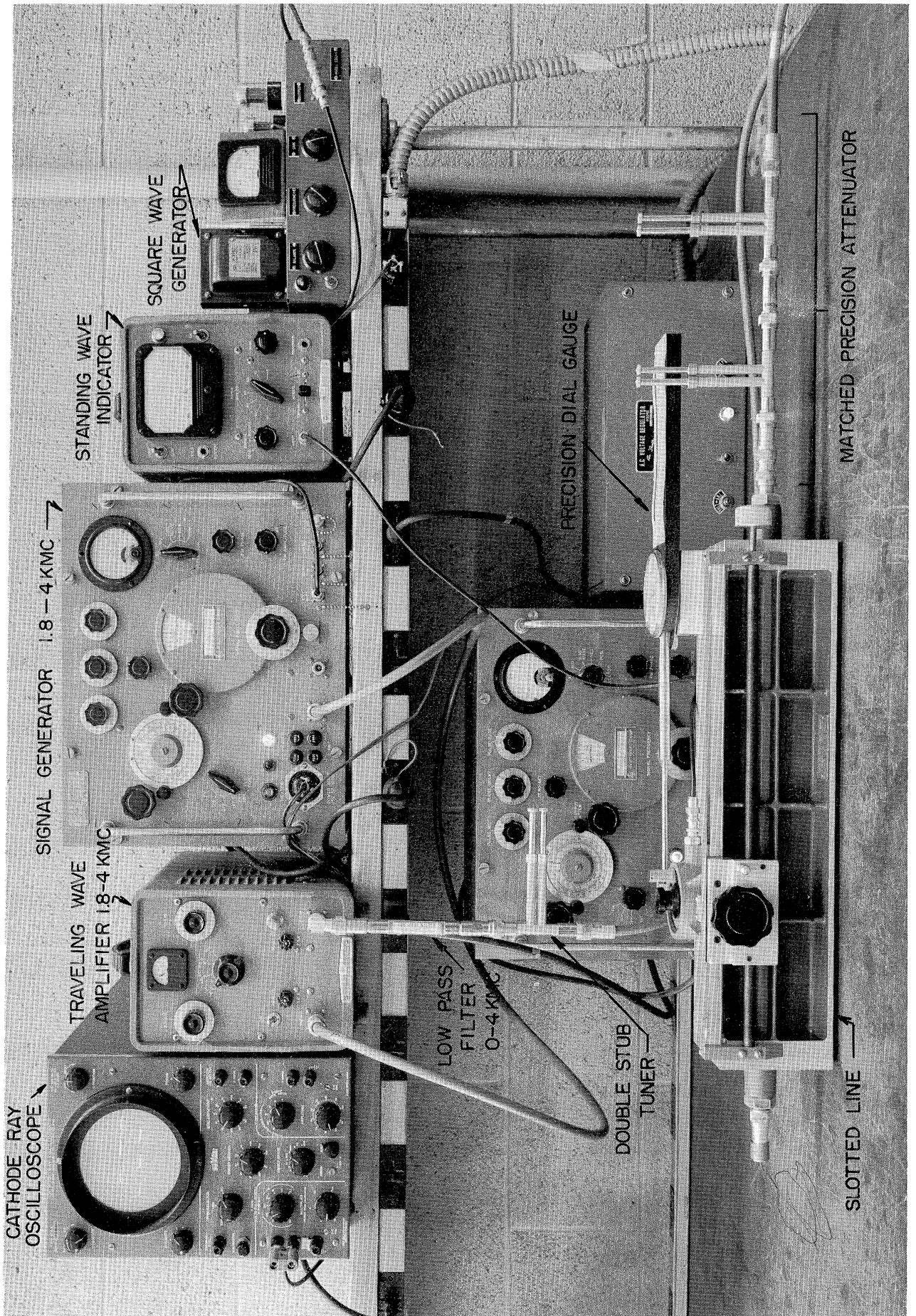


FIG 8 STANDING WAVE MEASUREMENT EQUIPMENT

Hewlett-Packard 616-A signal generator which has a frequency range of 1800-4000 mc. It is 100 per cent square wave modulated at the rate of 1000 cps by means of an externally generated signal. Its output is delivered to a Hewlett-Packard 491-A traveling wave amplifier which is capable of producing one watt of power over the frequency range of the signal generator. The amplifier output signal passes through a 0-4000 mc. low-pass filter so as to eliminate harmonic frequency components. A coaxial double-stub tuner is connected between the low-pass filter and the Hewlett-Packard 805-A slotted line, the latter being terminated in the load to be measured. The slotted line is also equipped with a dial gauge for the accurate measurement of linear displacements along the line. A clutch system permits a precision drive mechanism to be quickly engaged for accurate positioning of the detector head.

The detector output is delivered to the standing wave indicator when measurements are made. This indicator consists of a high gain audio amplifier whose output signal passes through a very narrow band filter, before reaching the meter. The center frequency of the filter is 1000 cps. The frequency of the square wave generator is established, therefore, by tuning for a maximum response on the standing wave indicator.

A provision also exists for radio frequency tuning of the detector on the slotted line. This can be accomplished according to a method described by Caicoya (Ref. 13), wherein a short circuit is placed on the line and the position of two convenient standing wave minima are located. The detector is then moved to the mid-point lying between these nulls and tuned for maximum meter indication.

In addition to the signal source and detecting apparatus, a cathode ray oscilloscope is also employed as shown in the photograph. After the equipment has been turned on for a sufficient time to stabilize, and before measurements are started, the oscilloscope is connected to the output of the detector on the slotted line. The gain control on the square wave generator, which modulates the signal source, is then adjusted to produce a modulation envelope, as observed on the scope, having flat tops and bottoms. This precaution avoids the generation of spurious signals; a condition which usually exists when the envelope shows evidence of sharp peaks in the modulation pattern (Ref. 73). The detector output is then reconnected to the standing wave indicator.

A fixed precision coaxial attenuator manufactured by the Polytechnic Research and Development Company is used for accurately determining selected points on the standing wave pattern. It is designed so that its dissipative attenuation (Ref. 51) remains constant over the frequency range of 1000-4000 mc. This is accomplished by controlling the thickness of the metallized resistive film, which is sprayed on the glass center rod, so that it is less than the skin depth for any frequency of operation.\* The dissipative attenuation is established within an uncertainty of  $\pm 0.20$  db at the calibration frequency.

At other frequencies the insertion loss differs from the dissipative attenuation as a consequence of the reflection arising from the type-N connectors and the adjoining network. Tomiyasu has shown (Ref. 66) that a linear passive bilateral network (such as the equivalent circuit which represents these attenuators at a single frequency) can be made to exhibit its minimum or intrinsic attenuation by the addition of suitable lossless network at each pair of network terminals. Thus, by employing double-stub tuners at each end of the precision coaxial attenuator, the dissipative attenuation can be achieved at any frequency.

The first step in the matching procedure, therefore, is the tuning operation which leads to a bilateral match of the precision coaxial attenuator. It has been pointed out (Ref. 25) that type-N coaxial connectors may give rise to reflections of 10 per cent with a consequent uncertainty in the resulting impedance measurement of 20 per cent or more. However, experience has shown that by carrying out the matching procedure with a double-stub tuner, at the particular connector where reflections must be eliminated, the uncertainty in the determination of impedance is very substantially decreased.\*\*

The second step in the matching procedure involves a tuning operation which provides for a complete elimination of reflections at the amplifier output terminals. Under typical circumstances, the traveling wave amplifier drives

---

\* PRD Microwave Equipment Catalog, Polytechnic Research and Development Company, Brooklyn, New York.

\*\* The main assumption made here is that both the connector and the double-stub tuner are lossless.

the slotted line through a low-pass filter and double-stub tuner,\* as shown in Fig. 8.

The slotted line is first terminated in a matched load and the amplifier potentials are adjusted to produce the required signal level. The matched load is then removed from the slotted line and the signal generator drive is removed from the traveling wave amplifier input. The load is connected to the amplifier input and the signal generator now drives the slotted line from the previously terminated end. The double-stub tuner at the amplifier output is adjusted to produce a perfect match as observed on the standing wave indicator. The equipment is subsequently reconnected as before in preparation for the standing wave measurement.

A careful examination of the foregoing procedure indicates that an assumption is made concerning the generator match. While the double-stub tuner is being adjusted, the amplifier input is terminated in a passive load so that a smooth unbunched electron beam passes through the helix. However, in performing the measurement the signal generator drives the amplifier input and normal bunching exists in the electron beam. A question might therefore be raised concerning the validity of the match under test conditions.

Inasmuch as small signal conditions apply to the one watt traveling wave amplifier in question, the rf variations may be regarded as small perturbations on the steady beam current. Accordingly, only small changes in the active output impedance of the amplifier may be expected during the measurement.

Dr. Lacy, of the Hewlett-Packard Company, has described one condition,\*\* however, which could affect the amplifier output impedance. A small but finite reverse beam current exists as a result of elastically reflected secondary electrons, causing regeneration (and hence a change of output impedance) at low signal levels. This beam should saturate far below forward beam saturation, perhaps 40 to 60 db down. Under normal circumstances, the output match should be well behaved above reverse beam saturation but below forward beam saturation.

---

\* The matched precision attenuator, shown connected between the amplifier output and the slotted line, will ordinarily be removed while the generator match is being performed.

\*\* Private communication.



The exact amount of reverse beam current, which varies among different tubes of the same design, would appear to be small for the particular traveling wave amplifier used here, owing to the close correlation of data obtained over a wide range of test conditions.

### 3.2 The Experimental Verification

Once the matching procedure has been carried out in accordance with the foregoing paragraph the standing wave ratio data is readily obtained. With the load, whose VSWR is to be determined, connected to the end of the slotted line the position of the minimum is found by selecting two equal-response points symmetrically located with respect to the minimum. The average of these two readings yields the desired point (References 6, 21, 25), at which the signal level of the minimum may be observed on the indicator. The precision coaxial attenuator, which has previously been matched at each end with double-stub tuners, is now inserted between the amplifier and the slotted line (as in Fig. 8). The traveling detector is now moved to a position along the line that yields the same reading on the indicator as before. The distance moved is known accurately from the dial gauge attached to the slotted line. The distance between successive minima yields the half-wavelength corresponding to the frequency of operation. This data, which includes  $x/\lambda$  and  $\alpha$ , suffices for obtaining the load VSWR from Fig. 6, or, with greater accuracy, from the standing wave chart located inside the back cover of this report.

Inasmuch as matched and short-circuited terminations are the only microwave coaxial standards commercially available, it has been necessary to apply a different line of reasoning in obtaining experimental verification of the method. Two types of test were employed: (1) the parameter variation test; and (2) the comparison test.

The parameter variation test makes use of the fact that if a large series of measurements are performed on the same unknown, each measurement differing from the others of the series only in the manner that the numerical data vary in accordance with a controlled change of a given parameter, the same final results must be obtained. In the present case the parameter most readily changed is the value of the fixed precision coaxial attenuator. Commercial models are manufactured having nominal attenuation values of 3, 6, 10

and 20 db. A record of such a series of measurements is given in Table II, for two different loads at an operating frequency of 3500 mc.

TABLE II  
PARAMETER VARIATION TEST

<u>Attenuation</u> db	<u>Measured</u> VSWR	<u>Attenuation</u> db	<u>Measured</u> VSWR
3.1	17.84	5.9	19.72
10.2	17.42	10.2	19.50
19.8	17.89	19.8	19.67

Within a certain degree of experimental error, it is clear from a study of the two loads examined that the measured standing wave ratio does not depend upon the value of attenuation used. The parameter variation test is thus fulfilled.

The comparison test is carried out by subjecting a given unknown load to at least two independent measurement processes. Agreement among the final results obtained from each of the procedures is then required. As pointed out earlier, the Winzemer method was investigated prior to the development of the rf substitution procedure. Accordingly, it was convenient to employ these two techniques for this test. A record of the results obtained for several different loads at an operating frequency of 3500 mc. is given in Table III.

In the case of the load whose VSWR is in the vicinity of 30:1 the results obtained by both methods are in good agreement. There is less variation, however, of the measured VSWR for the rf substitution method than for the Winzemer method.

The second load shows greater variation of the measured VSWR by either method. Both procedures lead to a VSWR in the vicinity of 51:1 when the 2.9 db attenuator is employed, while the remaining entries indicate a larger standing wave ratio. It would appear that even minor uncertainties in linear displacement measurements are significant when small angles are involved, since the Winzemer method does not require a knowledge of the attenuation used. However, uncertainty in attenuation does exert an influence upon the results obtained by the rf substitution method.

TABLE III  
COMPARISON TEST

Attenuation db	Measured Standing Wave Ratio	
	<u>Winzemer Method</u>	<u>RF Substitution Method</u>
2.9	31.23	29.72
5.9	29.98	29.35
10.2	30.32	29.21
19.8	29.45	29.16
2.9	51.64	51.36
5.9	55.29	53.81
10.2	54.89	53.87
19.8	55.42	53.61
2.9	182.57	185.66
5.9	182.57	181.82
10.2	187.58	187.43
19.8	211.87	180.96

The data pertaining to the third load shows some degree of variation by either technique, the closest correlation occurring for the 10.2 db attenuator, where the measured VSWR is nearly 187.5:1. The variations produced in the results of the rf substitution procedure are probably due principally to uncertainties arising from the attenuator mis-match errors, as described in the fourth chapter. The variations observed in the first three entries from the Winzemer method occur primarily as the result of uncertainties in the measurement of linear displacements.

It may also be noted that the result obtained for the Winzemer method, for the 19.8 db attenuator, is substantially greater than the remaining observations. The possible probe detuning, caused by a change of the crystal rectifier capacity leads to pattern distortion when large segments of the standing wave are examined.

## 4. ANALYSIS OF ERRORS

### 4.1 Fundamental Error Sources in Physical Measurement

Regardless of the amount of care exercised to minimize the error sources that exist in a measurement procedure, inevitable uncertainties, however small, will be present. After all precautionary steps have been taken, at least two types of error will remain:

(1) Field Perturbation Error - In order to perform any measurement, it is necessary to insert a suitable test device into the system to be observed. Its presence causes changes of such a nature that the actual observations differ from those which would be recorded if the instrument created no disturbance whatsoever.

In the case of the present investigation several factors contribute to this form of error. The presence of the slot, for example, causes a slight change in the electromagnetic field configurations in the slotted line as compared to the unslotted portions of the system. Also, radiant energy is lost through the slot; the exact amount depending upon the geometry of the system and the frequency of operation. The result of these influences is to cause a small change in the characteristic impedance of the transmission system and, in some circumstances, to give rise to the existence of slot waves (Ref. 45). It is also found that the velocity of propagation of the waves in the slotted section is slightly different from that of the unslotted section (Ref. 25).

The probe also creates a disturbance of the fields existing in the transmission system. If the dimensions of the probe are small compared to the wavelength (a condition usually satisfied in practice), it may be regarded as an equivalent lumped network shunting the line at the location of the probe (References 4, 6, 25, 45). In addition to the fact that the equivalent probe susceptance produces a shift in the positions of the standing wave maxima and minima (References 4, 13, 45), the observed standing wave ratio decreases with increasing probe conductance (References 45, 73). In some cases reflections from the probe may constitute an important disturbance (References 6, 50).

(2) The Display Error - This second form of error arises because it is impossible to construct truly ideal measurement equipment. For example, although barretters are designed to have a square law characteristic

over a wide dynamic range, small deviations from this type of response are known to exist. It follows, then, that the information presented to the observer differs from the actual physical conditions to which the readout equipment is subjected (even though field perturbations caused by the measurement equipment exist as described above) in a manner that is determined by the transfer function of the apparatus.

While the exact nature of both the field perturbation and the display errors introduced by the test equipment will depend largely upon the instruments and phenomena under investigation, all physical systems become subject to these limitations. It is only through the use of components of superior design and of highly refined experimental procedures that these disturbances can be kept at an absolute minimum.

## 4.2 Characteristics of the Slotted Line

Although several effects produced by typical slotted line equipment were briefly treated in the discussion of field perturbation errors, it is the purpose of this section to consider more carefully the characteristics of the actual test equipment.

4.2.1 Probe and Slot Effects. As shown in Fig. 8, the standing wave instrument employed is a Hewlett-Packard 805-A slotted line, to which a precision drive mechanism and dial gauge indicator have been attached. This particular apparatus was selected because it possesses several features which make it suitable for accurate standing wave measurements in coaxial transmission systems.

The ordinary type of coaxial slotted line (Ref. 45) consists simply of an additional portion of the coaxial system into which a slot is cut. This slot is oriented parallel to the lines of current flow, for the TEM mode of propagation, so as to minimize radiant energy. If the slot is relatively large, measurable energy is lost along the entire slot length, producing the effect of a distributed load upon the system (Ref. 75). In general, this "distributed load" has both real and imaginary components, so that an error results in processing experimental data if it is assumed that the characteristic impedance of the slotted section is purely resistive. In addition, the energy radiated from the slot is equivalent, as far as standing waves are concerned, to introducing uniform attenuation along the length of the system.

The standing wave ratio then depends upon the point at which the measurement is taken. This is one manifestation of "slope error;" the condition which exists when the observed standing wave ratio changes with position (Ref. 72).

If, on the other hand, the slot is made extremely narrow to minimize radiation, the slightest lateral motion of the probe due to mechanical imperfections will again lead to variations in the observed standing wave ratio with distance. This form of slope error arises because of changes of the probe-to-slot coupling (References 6, 21, 25, 45, 70, 72), or changes of probe-to-center conductor spacing, or changes of both. Mechanical difficulties which lead to a variation of probe penetration with detector motion produce a similar form of slope error.

In addition, eccentricity of the center conductor with respect to the outer conductor in the conventional coaxial line will create slight changes in the characteristic impedance of the system (Ref. 75). This is equivalent to producing slight discontinuities in an otherwise uniform line. Furthermore, even if perfectly axial motion of the detector is attained by mechanical means, the center conductor eccentricity will give rise to slope error.

It is probable that any given standing wave instrument, however carefully constructed, will exhibit several of these troublesome effects in varying degrees. The conventional slotted line is thus constrained by two conflicting requirements: (1) a narrow slot is necessary to prevent radiation and minimize slope error from this source; and, (2) a wide slot is necessary to prevent the slight lateral probe variations, due to mechanical imperfections, from causing this sort of slope error.

These disadvantages can be overcome by applying the widely known mathematical technique of conformal transformation to the usual type of coaxial transmission system, having a concentric center conductor. The result of one such transformation, after applying several minor modifications which facilitate fabrication, leads to the Hewlett-Packard 805-A slotted line (References 72, 75). The instrument has a wide natural slot which, when transformed back into the conventional coaxial geometry, is equivalent to a width of less than 0.002 radian. This small effective slot width is reported (Ref. 72) to have produced no discernible radiation. Furthermore, the configuration of the electric field lines in a typical cross section of the

slotted system is such as to make the changes of energy received by the probe much less sensitive to vertical and lateral variations than the conventional standing wave instrument.

A tapered section and matching network are employed to provide a smooth electrical transition between the coaxial and parallel-plane geometries. The success which has been achieved by these measures can be judged by the fact that a residual standing wave ratio as small as 1.01, at a single frequency, has been obtained (Ref. 72). These transitions can be made to produce reflections of less than 2 per cent over the equipment frequency range of 500 to 4000 mc. Commercial models are guaranteed to have a residual standing wave ratio of less than 1.04 over this range.

The technique used for examining these small residual reflections is that of the null shift procedure, originally developed by Feenberg (Ref. 22), and described in the first chapter of this report. A calibration procedure has been described by Oliner (Ref. 46) that can be used to correct the observed VSWR and the location of the standing wave minimum to account for the discontinuities introduced by the slot and the coaxial connectors. The method has not been applied to the measurements performed at this University since large standing wave ratios are the principal concern here. The residual VSWR quoted by the manufacturer would therefore be expected to produce only negligible effects upon the observations, over the indicated range of interest.

A study of the structural defects of the slotted line in determining the maximum errors in the measured VSWR and in the location of the minimum position was made by Ellenwood, Sorrows and Ryan (Ref. 21). Their results permit the evaluation of these maximum errors from data taken on the slotted line itself. The significance of these uncertainties assumes greater proportions as the standing wave ratio of the load approaches unity. Their analysis also shows that the nodal position error is minimized by selecting equal response points according to the relation

$$|V| = |V_{\min}| \sqrt{\frac{2\rho^2(\epsilon^2 - 1)}{\rho^2 + 1}}, \quad (27)$$

where

$$|V| = \text{magnitude of the voltage at the equal response points,}$$

$|V_{\min}|$  = magnitude of the voltage at the minimum,

$\rho$  = standing wave ratio, and

$\epsilon$  = fractional error of the voltage measurement in the slotted line due to inevitable structural imperfections.

A study of this equation shows that when the standing wave ratio approaches infinity the equal response voltages which minimize the error in the nodal position is equal to  $\sqrt{2}$  times the voltage at the standing wave minimum.

In paragraph 4.1 it was mentioned that the velocity of propagation of the waves in the slotted section of a coaxial (or waveguide) transmission system differs from that of the unslotted portions of the same system. For a given frequency, this leads to a corresponding change in the guided wavelength, which is larger in the slotted than in the unslotted region. However, the increase is small, often being less than one per cent (Ref. 45). Furthermore, since both  $x$  and  $\lambda$  are measured in the slotted line, each of these quantities is increased in the same proportion, so that no error should result from using  $x/\lambda$ , as measured on the slotted line, when the standing wave ratio is determined.

While few observations were made on the slot and coaxial connectors, somewhat greater attention was devoted to the influence of the probe upon the resulting measurements. The first consideration to be studied in this connection was that of the proper probe tuning procedure. The necessity for its correct adjustment has been long recognized (References 4, 45), but the method of accomplishing it has only recently been described (Ref. 13), as explained in the third chapter.

When a barretter is used as the detecting element, this technique yields the correct alignment even though the probe measurements are carried out in the vicinity of the standing wave minimum,\* regardless of the rf signal level that is applied to the slotted line.

---

\* It will be recalled that the probe tuning, described in the third chapter, is actually performed at a standing wave maximum.



If a crystal rectifier\* is used as the detecting element, however, additional care may sometimes be required to achieve the proper results. When large signal levels exist, such as those produced by a one watt traveling wave amplifier, the electric field intensity at a standing wave maximum is much greater than when only the relatively small signal levels from the ten milliwatt signal generator drive the system. In the presence of such large signals, the dynamic range to which the crystal rectifier is subjected, when it is tuned at the maximum and moved to the minimum position to perform standing wave measurements, is sufficiently large to cause severe mis-tuning at the location of the minimum. This is apparently due to a change of the barrier layer capacity which occurs when the crystal rectifier is subjected to large changes of field intensity, as described previously.

An approximate method, which appears to be better suited to existing test conditions, has been used at this University. A large, but finite, standing wave ratio is first created by inserting a double-stub tuner between a matched load and the terminating end of the slotted line, so that the signal level at the standing wave minimum is just discernible on the indicator. The rf tuning control on the detector head attached to the slotted line is then adjusted for a maximum response with the probe positioned at this "apparent" minimum location.\*\* Since the true minimum is slightly displaced from the point at which the probe is initially tuned, the detector is moved slightly in search of a smaller reading on the indicator. The tuning control is then re-adjusted to give a maximum meter response. Although, in principle, an infinite number of repetitions of the procedure are required to achieve the correct tuning, it is found that the process rapidly converges, so that relatively few re-adjustments are necessary.

The rf substitution procedure employed here, and described in the third chapter, makes use of the fact that the same signal level is applied to

---

\* The detecting elements used in this laboratory are the Sperry Type 821 barretter and the Sylvania Type 1N21C crystal rectifier.

\*\* It is recognized, of course, that this is not the true position of the standing wave minimum, because the probe susceptance causes a shift in the location of the minimum (Ref. 45). However, it is generally true that the minimum is shifted much less than the maximum by a given probe susceptance.

the probe before and after the insertion of the calibrated attenuator. Thus, by carrying out the above tuning procedure, errors due to an improperly tuned probe are eliminated.

When test conditions permit the use of the small signal levels developed by the ten milliwatt signal generator, the tuning of the probe and crystal rectifier detecting element may be carried out according to the procedure described earlier. Under these circumstances, the change in the electric field intensity to which the detector is subjected, when it is tuned at a maximum, is not sufficient to cause observable changes in alignment when measurements are made in the vicinity of the minimum.

The question of the proper probe depth has also been discussed by several authorities (References 4, 6, 45, 73). If the probe is withdrawn too far, even minor variations of the probe depth as the detector is moved, due to mechanical difficulties, will constitute a significant percentage of the indicator reading (Ref. 6). This follows from the fact that the magnitude of the mechanical variation of the probe penetration with motion is independent of the probe depth, while the indicator reading is exponentially proportional to penetration for the Hewlett-Packard slotted line (Ref. 25). Furthermore, insufficient probe depth leads to a severe degradation of the signal-to-noise ratio of the detector system. When the minimum is used for making standing wave measurement these effects become particularly important.

Alternatively, if the probe penetrates deeply, errors in the measurement of the VSWR and the nodal position may be pronounced, although, correction procedures are available (References 4, 45). It is frequently desirable, however, to avoid large probe penetrations.

One method for determining if the penetration is sufficiently large to cause serious distortion of the standing wave pattern is to place two identical probes in the same slotted line (Ref. 21). Whenever the motion of either probe causes a change in the reading on the indicator connected to the other probe, whose position is held fixed at selected points on the standing wave pattern, excessive penetration exists. Using a procedure similar to this, but separating the probes as far as practical to avoid direct coupling

between them, it was found that when the movable probe was withdrawn half of the total distance\* no appreciable changes could be observed.

Another group of tests were conducted to determine the effect of probe depth on measured VSWR. It was found that when the rf substitution method, described in the third chapter, was used the observed standing wave ratio was independent of probe depth over the entire range of control of probe penetration. The measurements were made on a load having a standing wave ratio of approximately 14:1. From a study of these two types of tests the practice has been followed of withdrawing the probe half of its total range.

A final series of investigations were conducted to determine the effect of probe diameter on the observed standing wave ratio. Numerous tests were made using steel probes whose diameters are: 0.018", 0.0098" and 0.0059". In each case, the results agreed closely with corresponding data taken on the Hewlett-Packard probe of 0.060". Standing wave ratios as large as 40:1 at a ten centimeter wavelength were measured using the rf substitution principle.

A rather interesting feature of these results is the fact that good correlation was obtained for all of the probes employed, even though a vast difference exists between the surface resistivity of the steel probes and that of the manufacturer. The latter is silver plated, while the former contained no plating of any type.

#### 4.3 Errors Affecting the RF Substitution Method

Many of the equipment characteristics described in the foregoing paragraph would exert an influence upon the observed data, regardless of the method used for the measurement of standing wave ratio. There are, however,

---

\* The slotted line has provisions for adjusting the probe depth by means of a screw thread which is machined into the depth control. About twenty complete turns of the adjustment screw will raise the probe from its bottom-most position near the center conductor to the limits of mechanical engagement of the screw. Thus half-way withdrawal represents about ten turns.

additional considerations which must be investigated when an attempt is made to establish limits of uncertainty for the rf substitution procedure. It is the purpose of this section to study the conditions which have a direct bearing on the present measurement technique.

4.3.1 Mismatch Errors. A study of the potential error sources, which may influence accuracy of the rf substitution technique, shows that they can be broadly divided into two categories: (1) the uncertainty of results which occur when the actual test equipment departs slightly from the prescribed theoretical conditions; and (2) the uncertainty of results which occur due to the inaccuracy of the readout equipment. Measurement errors attributable to the first category are treated in this section, while those of the second category are treated in the following section.

The principal factors which cause the actual test equipment to depart from the prescribed theoretical conditions are leakage radiation and improperly matched components (Ref. 51). Leakage radiation can be particularly troublesome since it may by-pass certain portions of the system and re-enter the test environment, producing uncontrolled disturbances. Erratic and seemingly contradictory behavior often result when such radiation, being signally-coherent with that portion of the energy under the influence of the operator, produces interference with the desired signal.

Leakage radiation can frequently be detected by making a series of observations on the same unknown, with only the physical disposition of equipment altered for each test in the sequence. After the precaution is taken to properly secure all mechanical and electrical connections prior to recording each set of measurements, a lack of agreement among the data, or erratic variations, often indicate the presence of leakage.

Numerous tests of this type were conducted during the early stages of experimentation. Quite naturally, the recommendations of the manufacturer were carefully followed. An analysis of the results showed that leakage radiation produced no measurable effects in so far as the equipment employed in the present work was concerned. For this reason, the main objective of this section is to focus attention upon the errors arising from the use of mis-matched components.

The importance of mis-match errors in microwave attenuation measurements is well recognized (Ref. 45). Since measurements involving known attenuation are used to determine standing wave ratios, according to the procedure discussed in this report, much of the knowledge acquired from attenuation studies can be directly applied here. One important analysis of effect of mis-match errors upon substitution measurements was presented by Beatty (Ref. 9).

In order to explain the significance of his results in the present investigation, let the functional arrangement of test equipment, shown in Fig. 8, be represented symbolically as in Fig. 9.

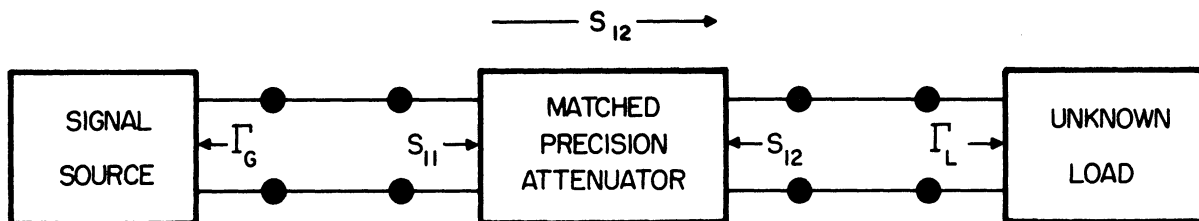


FIG. 9 BLOCK DIAGRAM REPRESENTATION OF RF SUBSTITUTION METHOD OF MEASURING STANDING WAVE RATIO

The symbols used in the above diagram are defined as follows:

$\Gamma_G$  = complex reflection coefficient of the signal source,

$\Gamma_L$  = complex reflection coefficient of the unknown load,

$S_{11}$  = complex reflection coefficient at the attenuator input when the attenuator output is match-terminated,

$S_{22}$  = complex reflection coefficient at the attenuator output when the attenuator input is match-terminated.

The quantities  $S_{11}$  and  $S_{22}$  are recognized to be the coefficients of the scattering matrix for the input and output ends of the attenuator, respectively (Ref. 45). In addition, the quantity  $S_{12}$  is the scattering matrix coefficient which relates the incident component of electric field intensity at

the source end of the attenuator to the incident component of the electric field intensity at the load end of the attenuator. A similar definition holds for  $S_{21}$  in terms of the reflected electric field intensities at the load and source ends of the same attenuator.

The network representing the precision attenuator will be symmetrical (Ref. 45) if

$$S_{11} = S_{22} \quad ,$$

and reciprocity holds (Ref. 45) if

$$S_{12} = S_{21} \quad .$$

The symmetry condition is achieved in the present case by employing double-stub tuners at each end of the attenuator, thus giving\*

$$S_{11} = S_{22} = 0 \quad .$$

Since the attenuators are linear, passive, bilateral networks the reciprocity condition is automatically satisfied.

Beatty has shown (Ref. 9) that the insertion loss,  $L$ , of the attenuator network differs from dissipative attenuation,  $\alpha$ , according to the relation

$$L = \alpha + \Delta\alpha$$

$$= -20 \log_{10} |S_{12}| + 20 \log_{10} \frac{|(1-S_{11}\Gamma_G)(1-S_{22}\Gamma_L) - S_{12}^2\Gamma_G\Gamma_L|}{|1 - \Gamma_G\Gamma_L|} \text{ db.} \quad (28)$$

---

\* Inspection of Fig. 9 shows that the scattering coefficient  $S_{11}$  is not observed at the attenuator input terminals during the substitution measurement, owing to reflections from the unknown load. However, it is assumed that the attenuator has previously been matched with a double-stub tuner at the input while its output is match-terminated, as described in the third chapter. Thus, the quantity  $S_{11}$  does in fact exist and is made equal to zero by the tuning procedure.

The quantity  $\Delta\alpha$  is a measure of the error experienced when  $\alpha$  is recorded instead of  $L$ . Inspection of this equation shows that  $\Delta\alpha$  can be reduced to zero if

$$S_{11} = S_{22} = \Gamma_G = 0 \quad ,$$

regardless of the magnitude of the load reflection coefficient. Thus, double-stub tuners are required at each end of the precision attenuator to constrain  $S_{11}$  and  $S_{22}$  to zero, while an additional double-stub tuner is required at the output of the traveling wave amplifier to make  $\Gamma_G$  equal zero. Upon carrying out the matching procedure described in the third chapter, standing wave ratios of less than 1.01 have been consistently obtained for the attenuator and signal source circuits.

Experience gained in this laboratory also indicates that another precaution must be observed when attempting to achieve the perfect match conditions described above. In each case, the double-stub tuning must be performed at the particular connector where the cancellation of reflections is desired. Experimental evidence shows that when such a tuning procedure is carried out at a given coaxial connector, and the tuner is subsequently moved to another connector of the same type, i.e., both connectors are either male or female, the match no longer holds. One such observation involving two female type-N connectors showed that after the desired match had been obtained at the first connector, a VSWR of 1.15 was observed at the second connector. Of course, upon re-adjustment of the tuner at the second connector the match condition was regained. It is nevertheless evident that minor constructional imperfections can create sufficient differences in the electrical behavior of apparently identical connectors as to invalidate the assumption that the match is invariant to all connectors of the same type.

Related studies have also shown that, when circumstances make it necessary, the tuner can be disassembled from and re-assembled\* to the same

---

\* It is assumed, of course, that the position of the tuning stubs are not disturbed. Usually this requires very careful handling. The task is greatly simplified when locking screws are used, such as those shown in Fig. 9.

coaxial junction without affecting the match. The retrieval of the match is, however, contingent upon properly re-tightening the junction.

In the course of the foregoing discussion it has been assumed that the double-stub tuners are entirely lossless. It has been pointed out by Mr. R. W. Beatty,\* of the National Bureau of Standards, that this condition is not fulfilled and that the tuner loss would have to be repeatable at each frequency, if an attempt is made to calibrate the matched attenuators against a primary standard. The calibration would have to be accomplished with the double-stub tuners properly adjusted at each calibration frequency and permanently attached to the associated attenuator.

It is quite apparent that the practice of first matching out the attenuator and then using the manufacturer's name plate data, which holds at only one frequency within the range of the device, leads to an uncertainty in the determination of  $\alpha$ . This inaccuracy is a form of display error that can be reduced only by further improvements in equipment design. A study of the sensitivity of VSWR computations to variations in  $\alpha$  has been made and the results are given in the following section.

The data presented in the third chapter also suggest that when standing wave ratios in excess of several hundred are encountered, it may be desirable to employ attenuations of 30 db or more in order to obtain suitable ranges of  $x/\lambda$ . It might appear that two or more attenuators could first be cascaded and then matched with tuners as described above. It would be incorrect, however, to take the total attenuation as equal to the sum of the attenuations of the separate devices, since an uncertainty arises due to an interaction of reflections (Ref. 7). Rinkel and Waller (Ref. 51) cite one such example, taken from Beatty's work, in which standing wave ratios of 1.2 and 1.5 produce an uncertainty of  $\pm 0.16$  decibels due to this type of interaction.

Nevertheless, this should not be regarded as a limitation of the method, inasmuch as the construction of 40 or 60 db fixed coaxial attenuators does not appear to be an impractical engineering task.

---

\* Private communication.



4.3.2 Attenuation, Angle and Wavelength Errors. The uncertainty in results which occurs as a consequence of the inaccuracy of the readout equipment is responsible for the display error present in the measurement. One form of this error arises because of an inexact knowledge of the value of the attenuation,  $\alpha$ , which applies in a specific test. The physical considerations which influence attenuator uncertainty have been described previously.

A second form of display error exists because small uncertainties exist in the measurement of linear displacements along the slotted line. These, in turn, result from small inaccuracies of the dial gauge readings. The two quantities affected by this error are the electrical angular displacement,  $\delta$ , which in the present case is measured relative to a standing wave minimum, and the wavelength,  $\lambda$ . The electrical angular displacement is related to the linear displacement,  $x$ , according to the relations stated in equations (15) and (16). It is the purpose of this section to investigate the changes which may be expected in the standing wave ratio,  $\rho$ , as the quantities  $\alpha$ ,  $x$  and  $\lambda$  are subjected to prescribed variations.

The total differential  $d\rho$  can be written

$$d\rho = \frac{\partial\rho}{\partial\alpha} d\alpha + \frac{\partial\rho}{\partial x} dx + \frac{\partial\rho}{\partial\lambda} d\lambda \quad , \quad (29)$$

which becomes approximately, upon using equation (22) and the following assigned increments:

$$\Delta\alpha = 0.20 \text{ decibel}, \quad \Delta x = \Delta\lambda = 0.01 \text{ millimeter},$$

$$\frac{\Delta\rho}{\rho} \approx \frac{0.01}{10^{\alpha/10} - \cos^2(2\pi x/\lambda)} \left[ (\ln 10)10^{\alpha/10} + \frac{(\pi/\lambda)(1-10^{\alpha/10})(1-x/\lambda)}{500 \tan(2\pi x/\lambda)} \right]. \quad (30)$$

This relation is an expression for the per unit uncertainty in standing wave ratio as a function of  $\alpha$ ,  $\lambda$  and  $x/\lambda$ . Table IV has been prepared with the aid of this result for a wavelength of ten centimeters.

TABLE IV  
STANDING WAVE RATIO UNCERTAINTY

$\lambda = 10$  centimeters

$\frac{(x)}{\lambda}$	$\alpha$ db	$\frac{\Delta\alpha}{\rho} \left( \frac{\partial \rho}{\partial \alpha} \right)$	$\frac{\Delta x}{\rho} \left( \frac{\partial \rho}{\partial x} \right)$	$\frac{\Delta\lambda}{\rho} \left( \frac{\partial \rho}{\partial \lambda} \right)$
0.001	3.01	0.04601	$9.99 \cdot 10^{-6}$	$-1 \cdot 10^{-8}$
0.010	3.01	0.04587	$9.95 \cdot 10^{-6}$	$-1 \cdot 10^{-7}$
0.100	3.01	0.03422	$6.42 \cdot 10^{-6}$	$-7.4 \cdot 10^{-7}$
0.001	6.02	0.03067	$9.99 \cdot 10^{-6}$	$-1 \cdot 10^{-8}$
0.010	6.02	0.03058	$9.95 \cdot 10^{-6}$	$-1 \cdot 10^{-7}$
0.100	6.02	0.02745	$7.73 \cdot 10^{-6}$	$-7.7 \cdot 10^{-7}$
0.001	9.03	0.02616	$11.36 \cdot 10^{-6}$	$-1 \cdot 10^{-8}$
0.010	9.03	0.02616	$11.34 \cdot 10^{-6}$	$-1 \cdot 10^{-7}$
0.100	9.03	0.02505	$9.41 \cdot 10^{-6}$	$-9.4 \cdot 10^{-7}$
0.001	21.07	0.02358	$10.24 \cdot 10^{-6}$	$-1 \cdot 10^{-8}$
0.010	21.07	0.02358	$10.23 \cdot 10^{-6}$	$-1 \cdot 10^{-7}$
0.100	21.07	0.02358	$8.86 \cdot 10^{-6}$	$-8.9 \cdot 10^{-7}$

The "most probable" uncertainty in standing wave ratio may be obtained by taking the square root of the sum of the squares of the absolute values of the separate entries in the table. When a large number of measurements are considered, this quantity is usually of interest. For a single observation, however, the algebraic sum of the terms is useful in specifying the bounds within which all uncertainties must exist.

In any event, the above table shows that the error produced in the standing wave measurement is almost completely determined by variations of attenuation. It may be observed that the uncertainty decreases from 4.6% for  $\alpha = 3.01$  db, to 2.358% for  $\alpha = 21.07$  db. This behavior is due to the fact

that the manufacturer establishes a fixed calibration uncertainty of  $\pm 0.20$  db for all sizes of attenuation.

The direct dependence of error in computed standing wave ratio upon attenuation shows that precise results can be expected only if carefully matched attenuators are used. Mr. Beatty has suggested\* that the calibration of precision attenuators, having a substantially reduced mis-match (without double-stub tuners), would lead to improved results. It is the author's understanding that such components are commercially available.

#### 4.4 The Effects of Frequency Drift

An important consideration which often arises when precision measurements are undertaken is the question of the frequency stability of the signal source. During preliminary stages of the present study, frequency shifts were observed to produce changes in wavelength of the order of 0.01 millimeters. These wavelength changes were ascertained from measurements carried out at half-hour intervals, after an initial warm up period of one hour or more.

Variations of wavelength of this magnitude have an important bearing upon the position of the standing wave minimum and, hence, the phase angle of the complex reflection coefficient. In addition, the shifts also affect the accuracy of the VSWR measurement and, therefore, the magnitude of the complex reflection coefficient. It would evidently be meaningless to attempt readings of linear displacements of 0.001 millimeters when frequency changes can produce uncertainties ten times as large.

Furthermore, such frequency drifts may result in a sufficient degree of mis-tuning of the double-stub tuners, on the attenuator and generator output, as to raise serious doubt concerning the validity of the matching procedure. The mis-alignment of the detector head on the slotted line, which also accompanies these frequency changes, may give rise to significant distortion of the standing wave pattern and concomittant measurement errors.

A careful study of the equipment characteristics and the prevailing laboratory conditions revealed that a major part of this frequency drift was

---

\* Private communication.

directly related to slight voltage variations of the 110 volt, 60 cps, ac supply. A small proportion of the frequency change could also be associated with the transient conditions to which the signal generator is subjected during warm up periods.

It was thus found that these detrimental frequency variations could be reduced below observable limits by interposing a line voltage regulator between the 60 cps supply and the microwave signal generator, as shown in Fig. 8. Moreover, whenever very precise measurements are involved, the signal generator is permitted two to four hours to stabilize.

## REFERENCES

The impedance measurement techniques employed in the microwave frequency range have been treated extensively. Special VSWR measurement procedures have sometimes been devised as part of a more general study relating to antennas, dielectrics and other electrical components. It has not always been possible, therefore, to cite work exclusively devoted to standing wave measurements.

1. Allen, C. P., and Lindsay, P. A., "Some Aspects of Standing Wave Patterns," Wireless Engineer, Vol. 32, No. 9, pp. 239-245, September, 1955.
2. Allen, P. J., "An Automatic Standing Wave Indicator," Electrical Engineering, Vol. 67, No. 11, p. 1082, November, 1948.
3. Allred, C. M., "Chart for TE<sub>11</sub> Mode Piston Attenuator," Electronics, Vol. 26, No. 1, p. 142, January, 1953.
4. Altar, W., Marshall, R. B., and Hunter, L. P., "Probe Errors in Standing Wave Detectors," Proc. IRE, Vol. 34, No. 1, pp. 33P-44P, January, 1946.
5. Altshuler, J., "Attenuators with Mismatched Terminations," Wireless Engineer, Vol. 33, No. 11, pp. 257-258, November, 1956.
6. Barlow, H. M., and Cullen, A. L., Microwave Measurements, Constable and Company, Ltd., London, 1950.
7. Beatty, R. W., "Cascade-Connected Attenuators," Journal of Research of the National Bureau of Standards, Vol. 45, No. 3, pp. 231-235, September, 1950.
8. Beatty, R. W., "Determination of Attenuation from Impedance Measurements," Proc. IRE, Vol. 38, No. 8, pp. 895-897, August, 1950.
9. Beatty, R. W., "Mismatch Errors in the Measurement of Ultra-High Frequency and Microwave Variable Attenuators," Journal of Research of the National Bureau of Standards, Vol. 52, No. 1, pp. 7-9, January, 1954.
10. Beatty, R. W., and MacPherson, A. C., "Mismatch Errors in Microwave Power Measurements," Proc. IRE, Vol. 41, No. 9, pp. 1112-1119, September, 1953.
11. Beatty, R. W., and Reggia, F., "Characteristics of the Magnetic Attenuator at UHF," Proc. IRE, Vol. 41, No. 1, pp. 93-100, January, 1953.
12. Bloch, A., Fisher, F. J., and Hunt, G. J., "New Equipment for Impedance Matching and Measurement at Very High Frequencies," Proc. IEE, Part III, Vol. 100, pp. 93-100, 1953.

13. Caicoya, J. I., "Tuning a Probe in a Slotted Line," Proc. IRE, Vol. 46, No. 4, pp. 787-788, April, 1958.
14. Chipman, R. A., "Resonance Curve Method for the Absolute Measurement of Impedance at Frequencies of the Order of 300 mc/second," Journal of Applied Physics, Vol. 10, No. 1, pp. 27-38, January, 1938.
15. Conley, P., "Antennas and Open Wire Lines, Part III: Image-Line Measurements," Journal of Applied Physics, Vol. 20, No. 11, pp. 1022-1026, November, 1949.
16. Dakin, T. W., and Works, C. N., "Microwave Dielectric Measurements," Journal of Applied Physics, Vol. 18, No. 9, pp. 789-796, September, 1947.
17. Deschamps, G. A., "Determination of Reflection Coefficient and Insertion Loss of a Waveguide Junction," Journal of Applied Physics, Vol. 24, No. 8, pp. 1046-1050, August, 1953.
18. Easton, I. G., "Measurements of the Characteristics of Transmission Lines," Parts I and II, General Radio Experimenter, Vol. 18, Nos. 6 and 7, November-December, 1943.
19. Ebert, J., "Metallized Glass Microwave Attenuators," PRD Reports, Vol. 1, No. 3, October, 1952.
20. Ellenwood, R. C. and Hurlburt, E. H., "The Determination of Impedance with a Double-Slug Transformer," Proc. IRE, Vol. 40, No. 12, pp. 1690-1693, December, 1952.
21. Ellenwood, R. C., Sorrows, H. E., and Ryan, W. E., "Evaluation of Co-axial Slotted Line Impedance Measurements," Proc. IRE, Vol. 39, No. 2, pp. 162-168, February, 1951.
22. Feenberg, E., "The Relation Between Nodal Positions and Standing Wave Ratio in a Composite Transmission System," Journal of Applied Physics, Vol. 17, No. 6, pp. 530-532, June, 1946.
23. Fong, A., "Direct Measurement of Impedance in the 50-500 Mc Range," Hewlett-Packard Journal, Vol. 1, No. 8, April, 1950.
24. Gainsborough, G. F., "A Method of Calibrating Standard Signal Generators and Radio Frequency Attenuators," Proc. IEE, Part III, pp. 203-210, May, 1947.
25. Ginzton, E. L., Microwave Measurements, McGraw-Hill Book Co., Inc., New York, 1958.
26. Gordon-Smith, A. C., "Calibrated Piston Attenuator," Wireless Engineer, Vol. 26, No. 10, pp. 322-324, October, 1949.
27. Grantham, R. E., "A Reflectionless Waveguide Termination," Review of Scientific Instruments, Vol. 22, No. 11, pp. 828-834, November, 1951.

28. Grantham, R. E., "Reducing Standing Waves," Electronics, Vol. 22, No. 1, p. 124, January, 1949.
29. Grantham, R. E., and Freeman, J. J., "Microwave Attenuation Standard," Electrical Engineering, Vol. 67, No. 6, pp. 535-537, June, 1948.
30. Harris, F. E., and O'Konski, C. T., "Measurement of High Permittivity Dielectrics at Microwave Frequencies," Review of Scientific Instruments, Vol. 26, No. 5, pp. 482-485, May, 1955.
31. Hirst, D., and Hogg, R. W., "The Design of Precision Standing-Wave Indicators for Measurement in Waveguides," Proc. IEE, Vol. 94, Part III-A, No. 14, 1947.
32. Hopfer, S., "Precision Measurements with Slotted Sections," PRD Reports, Vol. 2, No. 3, October, 1953.
33. Hopfer, S. A., and Finke, H. A., "Impedance Measurements in the 50-1000 mc/sec Range with a New Standing Wave Indicator," PRD Reports, Vol. 3, No. 2, January, 1955.
34. Hollum, A. G., Jr., "Complex Dielectric-Constant Measurements in the 100-to-1000 Megacycle Range," Proc. IRE, Vol. 38, No. 8, pp. 883-885, August, 1950.
35. King, D. D., "Impedance Measurements on Transmission Lines," Proc. IRE, Vol. 35, No. 5, pp. 509-514, May, 1947.
36. King, D. D., and King, R., "Microwave Impedance Measurements with Applications to Antennas, Parts I and II," Journal of Applied Physics, Vol. 16, No. 8, pp. 435-453, August, 1945.
37. King, R., "Antennas and Open Wire Lines, Part I: Theory and Summary of Measurements," Journal of Applied Physics, Vol. 20, No. 9, pp. 832-850, September, 1949.
38. Korewick, J., "AM System Measures Microwave Attenuation," Electronics, Vol. 27, No. 1, pp. 175-177, January, 1954.
39. Korewick, J., "Audio Modulation Substitution System for Microwave Attenuation Measurements," Trans. IRE, MTT-1, No. 1, pp. 14-21, March, 1953.
40. Laskin, H. J., "Microwave Detectors for Measurements at Relative Power Levels," PRD Reports, Vol. 3, No. 1, July, 1954.
41. MacPherson, A. C., and Kerns, D. M., "A New Technique for the Measurement of Microwave Standing-Wave Ratios," Proc. IRE, Vol. 44, No. 8, pp. 1024-1030, August, 1956.
42. Mathis, H. F., "Transmission Line Impedance Measurements," Electronics, Vol. 30, No. 6, p. 186, June, 1957.

43. Mathis, H. F., "Measurement of Reflection Coefficients Through a Lossless Network," Trans. IRE, MTT-3, No. 5, p. 58, October, 1955.
44. Medhurst, R. G., and Pool, S. D., "Correction Factors for Slotted Measuring Lines at Very High Frequencies," Proc. IEE, Part III, pp. 223-230, 1950.
45. Montgomery, C. G., Technique of Microwave Measurements, Vol. 11, MTT Rad. Lab. Series, McGraw-Hill Book Co., Inc., New York, 1947.
46. Oliner, A. A., "The Calibration of the Slotted Section for Precision Microwave Measurements," Review of Scientific Instruments, Vol. 25, No. 1, pp. 13-20, January, 1954.
47. Oliner, A. A., and Altschuler, H. M., "A Shunt Technique for Microwave Measurements," Trans. IRE, MTT-3, No. 4, pp. 24-30, July, 1955.
48. Parzen, P., "Matching Conditions in a Stub-Tuned Transmission Line," Proc. IRE, Vol. 35, No. 2, p. 170, February, 1947.
49. Redheffer, R. M., "Radome Bulletin No. 9: The Matching of High Standing Wave Ratios," M.I.T. Radiation Lab. Report No. 483-9, December 22, 1944.
50. Redheffer, R. M., and Dowker, Y., "An Investigation of RF Probes," M.I.T. Radiation Lab. Report No. 483-14, February 6, 1946.
51. Rinkel, S. A., and Waller, W. E., "Microwave Attenuation Measurements," PRD Reports, Vol. 4, No. 1, April, 1955.
52. Roberts, S., and von Hippel, A., "A New Method for Measuring Dielectric Constant and Loss in the Range of Centimeter Waves," Journal of Applied Physics, Vol. 17, No. 7, pp. 610-616, July, 1946.
53. Roof, J. G., "Transmission Loss Charts," Electronics, Vol. 17, No. 6, pp. 130-132, June, 1944.
54. Rosenthal, L. A., and Badoyannis, G. M., "Direct VSWR Readings in Pulsed RF Systems," Electronics, Vol. 27, No. 12, pp. 162-165, December, 1954.
55. Saito, S., and Kurokawa, K., "Precision Resonance Method of Measuring Dielectric Properties of Low Loss Solid Materials in the Microwave Range," Proc. IRE, Vol. 44, No. 1, pp. 35-42, January, 1956.
56. Schlicke, H. M., "Efficiency of Mismatched Lines," Electronics, Vol. 23, No. 6, pp. 114-116, June, 1950.
57. Selby, M. C., Wolzien, E. C., and Jickling, R. M., "Coaxial Radio-Frequency Connectors and Their Electrical Quality," Journal of Research of the National Bureau of Standards, Vol. 52, No. 3, pp. 121-132, March, 1954.



58. Soderman, R. A., "The Measurement of Dielectric Properties in the 200-5000 Mc Range," General Radio Experimenter, Vol. 32, No. 12, pp. 3-9, May, 1958.
59. Soderman, R. A., and Hague, W. M., "UHF Impedance Measurements with the Type 874-LB Slotted Line," General Radio Experimenter, Vol. 25, No. 6, November, 1950.
60. Stewart, C., Jr., "Electrical Testing of Coaxial Radio-Frequency Cable Connectors," Proc. IRE, Vol. 33, No. 9, pp. 609-619, September, 1945.
61. Surber, W. H., Jr., and Crouch, G. E., Jr., "Dielectric Measurement Methods for Solids at Microwave Frequencies," Journal of Applied Physics, Vol. 19, No. 12, pp. 1130-1139, December, 1948.
62. Teal, G. K., Rigterink, M. D., and Frosch, C. J., "Attenuator Materials, Attenuators and Terminations for Microwaves," AIEE Transactions, Vol. 67, Part I, pp. 419-428, 1948.
63. Thurston, W. R., "Simple Complete Coaxial Measuring Equipment for the UHF Range," General Radio Experimenter, Vol. 24, No. 8, January, 1950.
64. Tomiyasu, K., "Antennas and Open-Wire-Lines. Part II: Measurements on Two Wire Lines," Journal of Applied Physics, Vol. 20, No. 10, pp. 892-896, October, 1949.
65. Tomiyasu, K., "Loading and Coupling Effects of Standing-Wave Indicators," Proc. IRE, Vol. 37, No. 12, pp. 1405-1409, December, 1949.
66. Tomiyasu, K., "Intrinsic Insertion Loss of a Mismatched Microwave Network," Trans. IRE, MTT-3, No. 1, pp. 40-44, January, 1955.
67. van Hofweegen, J. M., "Impedance Measurements with a Non-Tuned Lecher System," Phillips Technical Review, Vol. 8, No. 9, pp. 278-286, September, 1946.
68. van den Hoogenband, J. C., and Stolk, J., "Reflection and Impedance Measurements by Means of a Long Transmission Line," Phillips Technical Review, Vol. 16, No. 11, pp. 309-320, May, 1955.
69. Vogelmann, J. H., "Precision Measurements of Waveguide Attenuation," Electronics, Vol. 26, No. 12, pp. 196-199, December, 1953.
70. Wareham, E. M., "Slotted Section Standing Wave Meter," Journal of the British IRE, Vol. 15, No. 11, pp. 539-564, November, 1955.
71. Westcott, C. H., "Standing Waves and Impedance Circle Diagrams," Wireless Engineer, Vol. 26, No. 7, pp. 230-234, July, 1949.
72. Wholey, W. B., "Greater Reliability in UHF Impedance Measurements," Hewlett-Packard Journal, Vol. 1, No. 5, January, 1950.

73. Wholey, W. B., "Good Practice in Slotted Line Measurements," Hewlett-Packard Journal, Vol. 3, Nos. 1-2, September-October, 1951.
74. Wholey, W. B., and Hunton, J. K., "The 'Perfect Load' and the Null Shift - Aids in VSWR Measurements," Hewlett-Packard Journal, Vol. 3, Nos. 5-6, January-February, 1952.
75. Wholey, W. B., and Eldred, W. N., "A New Type of Slotted Line Section," Proc. IRE, Vol. 38, No. 3, pp. 244-248, March, 1950.
76. Wing, A. H., and Eisenstein, J., "Single- and Double-Stub Impedance Matching," Journal of Applied Physics, Vol. 15, No. 8, pp. 615-622, August, 1944.
77. Winzemer, A. M., "Methods for Obtaining the Voltage Standing-Wave Ratio on Transmission Lines Independently of the Detector Characteristics," Proc. IRE, Vol. 38, No. 3, pp. 275-279, March, 1950.
78. \_\_\_\_\_, Notes on Microwave Measurements, Polarad Electronics Corporation, New York, 1958.
79. \_\_\_\_\_, Weinschel Engineering and Application Notes, Weinschel Engineering Company, Kensington, Maryland, 1958.

DISTRIBUTION LIST

1 Copy Document Room  
Stanford Electronic Laboratories  
Stanford University  
Stanford, California

1 Copy Commanding General  
Army Electronic Proving Ground  
Fort Huachuca, Arizona  
Attn: Director, Electronic Warfare Department

1 Copy Chief, Research and Development Division  
Office of the Chief Signal Officer  
Department of the Army  
Washington 25, D. C.  
Attn: SIGEB

1 Copy Chief, Plans and Operations Division  
Office of the Chief Signal Officer  
Washington 25, D. C.  
Attn: SIGEW

1 Copy Countermeasures Laboratory  
Gilfillan Brothers, Inc.  
1815 Venice Blvd.  
Los Angeles 6, California

1 Copy Commanding Officer  
White Sands Signal Corps Agency  
White Sands Proving Ground  
Las Cruces, New Mexico  
Attn: SIGWS-EW

1 Copy Commanding Officer  
White Sands Signal Corps Agency  
White Sands Proving Ground  
Las Cruces, New Mexico  
Attn: SIGWS-FC

1 Copy Commanding Officer  
Signals Corps Electronics Research Unit  
9560th USASRU  
Mountain View, California



65 Copies	Transportation Officer, SCEL Evans Signal Laboratory Building No. 42, Belmar, New Jersey
	FOR - SCEL Accountable Officer Inspect at Destination File No. 22824-PH-54-91(1701)
1 Copy	H. W. Farris University of Michigan Research Institute University of Michigan Ann Arbor, Michigan
1 Copy	Technical Documents Services Willow Run Laboratories Building 255 University of Michigan Ypsilanti, Michigan
12 Copies	Electronic Defense Group Project File University of Michigan Ann Arbor, Michigan
1 Copy	University of Michigan Research Institute Project File University of Michigan Ann Arbor, Michigan